UC Davis

UC Davis Previously Published Works

Title

The microtubular preprophase band recruits Myosin XI to the cortical division site to guide phragmoplast expansion during plant cytokinesis

Permalink

https://escholarship.org/uc/item/8f03j612

Authors

Huang, Calvin Haoyuan

Peng, Felicia Lei

Lee, Yuh-Ru Julie

et al.

Publication Date

2024-06-01

DOI

10.1016/j.devcel.2024.05.015

Copyright Information

This work is made available under the terms of a Creative Commons Attribution License, available at https://creativecommons.org/licenses/by/4.0/

Peer reviewed

eScholarship.org Powered by the California Digital Library
University of California

Article

Developmental Cell

The microtubular preprophase band recruits Myosin XI to the cortical division site to guide phragmoplast expansion during plant cytokinesis

Graphical abstract

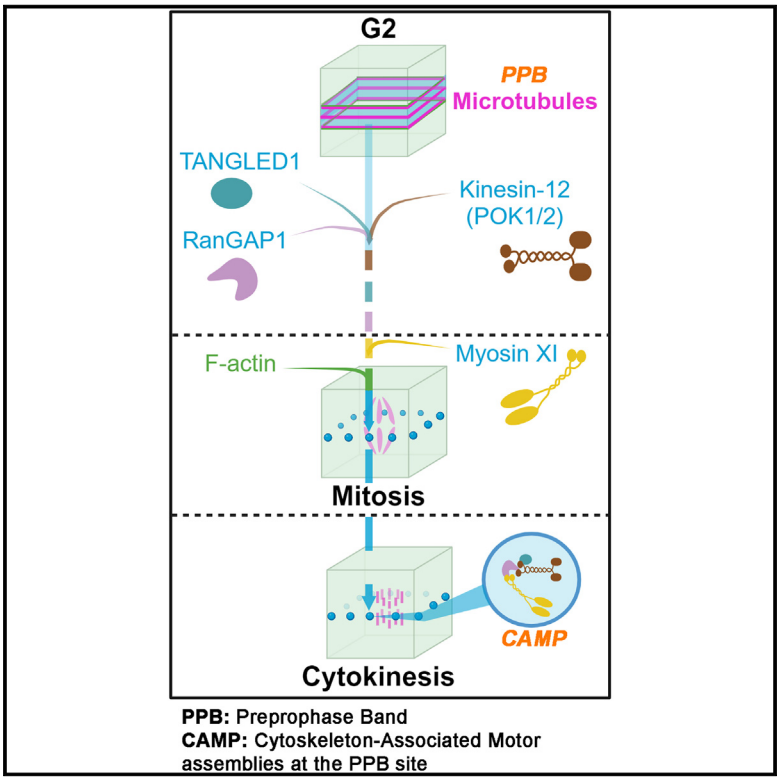

PPB: Preprophase Band
CAMP: Cytoskeleton-Associated Motor assemblies at the PPB site

Highlights

- Microtubule preprophase band (PPB) recruits myosin XI to the cortical division site
- Myosin XI and kinesin-12 are in the cytoskeleton-associated motor assemblies (CAMPs)
- F-actin is required for CAMP development into discrete cortical foci at late mitosis
- CAMPs translate PPB into the phragmoplast fusion/cell plate insertion site for cytokinesis

Authors

Calvin Haoyuan Huang, Felicia Lei Peng, Yuh-Ru Julie Lee, Bo Liu

Correspondence

bliu@ucdavis.edu

In brief

Cell division plane orientation in flowering plants requires orchestrated actions of microtubules and F-actin. Huang et al. find that myosin XI and kinesin-12 form discrete F-actin-dependent cytoskeletal motor assemblies that translate the microtubule preprophase band into the cortical division site to guide phragmoplast expansion and cell plate insertion during cytokinesis.

Huang et al., 2024, Developmental Cell *59*, 1–14
September 9, 2024 © 2024 Elsevier Inc. All rights are reserved, including those for text and data mining, AI training, and similar technologies.
https://doi.org/10.1016/j.devcel.2024.05.015

CellPress

Please cite this article in press as: Huang et al., The microtubular preprophase band recruits Myosin XI to the cortical division site to guide phragmoplast expansion during plant cytokinesis, Developmental Cell (2024), https://doi.org/10.1016/j.devcel.2024.05.015

Developmental Cell

CellPress

Article

The microtubular preprophase band recruits Myosin XI to the cortical division site to guide phragmoplast expansion during plant cytokinesis

Calvin Haoyuan Huang,[1] Felicia Lei Peng,[1,2] Yuh-Ru Julie Lee,[1] and Bo Liu[1,3,*]
[1]Department of Plant Biology, College of Biological Sciences, University of California, Davis, CA 95616, USA
[2]Present address: Department of Genetics, Perelman School of Medicine, University of Pennsylvania, Philadelphia, PA 19104, USA
[3]Lead contact
*Correspondence: bliu@ucdavis.edu
https://doi.org/10.1016/j.devcel.2024.05.015

SUMMARY

In plant vegetative tissues, cell division employs a mitotic microtubule array called the preprophase band (PPB) that marks the cortical division site. This transient cytoskeletal array imprints the spatial information to be read by the cytokinetic phragmoplast at later stages of mitotic cell division. In *Arabidopsis thaliana*, we discovered that the PPB recruited the Myosin XI motor MYA1/Myo11F to the cortical division site, where it joined microtubule-associated proteins and motors to form a ring of prominent cytoskeletal assemblies that received the expanding phragmoplast. Such a myosin localization pattern at the cortical division site was dependent on the POK1/2 Kinesin-12 motors. This regulatory function of MYA1/Myo11F in phragmoplast guidance was dependent on intact actin filaments. The discovery of these cytoskeletal motor assemblies pinpoints a mechanism underlying how two dynamic cytoskeletal networks work in concert to govern PPB-dependent division plane orientation in flowering plants.

INTRODUCTION

Plant growth is dependent on the production of new cells in physiologically informative orientations in order to build tissues in a spatially regulated manner, in part because plant cells are constrained by the rigid cell wall that prevents cell locomotion. From embryogenesis to organogenesis, plant cytokinesis employs a transient microtubule-based cytoskeletal array called the preprophase band (PPB) at the cell cortex. The PPB emerges during the G2 phase, matures in prophase to demarcate the division site, and is disassembled concomitantly with nuclear envelope breakdown (NEB) toward the end of prophase.[1] During vegetative growth, the PPB is employed during both proliferating divisions to produce more identical cells and formative division to produce two daughter cells with distinct fates. The PPB-demarcated cortical division site (CDS) is read by the cytokinetic apparatus phragmoplast so that the cell plate synthesized by the latter will be inserted into the plasma membrane at the CDS to partition the two daughter cells. The PPB is therefore of paramount importance for robust tissue generation and growth throughout the life of a plant.[2]

Previously, a pharmacological study informed us that the translation of the PPB microtubule array into the CDS after PPB disassembly is dependent on actin microfilaments (F-actin) in plant cells.[3] F-actin is detected in the PPB at early stages of its development but disappears from the mature PPB and is undetectable at the CDS.[4] The nature of the role that F-actin plays in guiding the expanding phragmoplast to precisely recognize the cell plate fusion site at later stages of cell division has been enigmatic.[5] In the meantime, proteins like the microtubule-associated protein TANGLED1 (TAN1) and its interacting Kinesin-12 motor phragmoplast orienting kinesin 1 (POK1) persist at the CDS after PPB disassembly and play critical roles in the maintenance of the CDS established by the PPB.[6,7] However, in the context of cell division plane determination, it remains unclear how the function of these microtubule-associated factors is integrated with that of F-actin.

The crosstalk between the two cytoskeletal systems during plant cell division may be mediated by myosin motors, as evidenced by the phragmoplast microtubule association of the Myosin VIII motors in the moss *Physcomitrium patens* and Myosin XI -K/Myo11E in the angiosperm *Arabidopsis thaliana* (*A. thaliana*).[8,9] In these two plant models, simultaneous losses of multiple Myosin VIII and Myosin XI, respectively, led to mild division plane misalignment phenotypes. In *A. thaliana*, different Myosin XI isoforms, including Myosin XI-K/Myo11E and MYA1/Myo11F, were predicted to acquire specialized functions due to the diversification of their sequences and enzymatic properties.[10,11] A study reported that F-actin generates the force for the development of the narrow (mature) PPB microtubule array from a wide one.[12] Therefore, we hypothesized that actin-based motors play critical roles in division plane orientation and that functionally redundant Myosin XI motors mediated the actin-microtubule interaction at the cell

All rights are reserved, including those for text and data mining, AI training, and similar technologies.

Please cite this article in press as: Huang et al., The microtubular preprophase band recruits Myosin XI to the cortical division site to guide phragmoplast expansion during plant cytokinesis, Developmental Cell (2024), https://doi.org/10.1016/j.devcel.2024.05.015

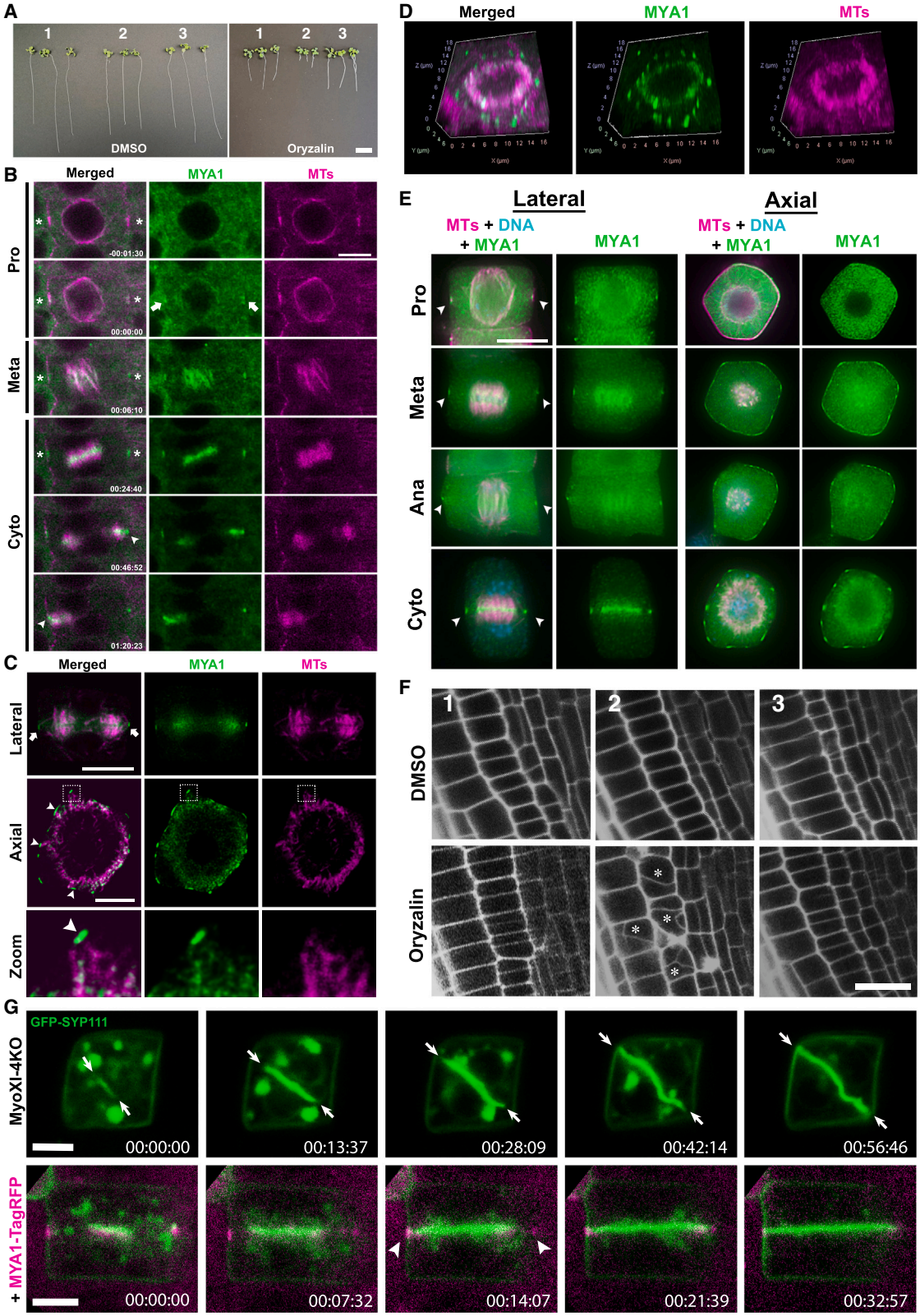

Figure 1. The Myosin XI motor MYA1 decorates the cortical division site and plays a critical role in cell division plane determination in *A. thaliana*

Scale bars: 1 cm in (A), 5 μm in (B), (C), (E), and (G), and 20 μm in (F).

(legend continued on next page)

Please cite this article in press as: Huang et al., The microtubular preprophase band recruits Myosin XI to the cortical division site to guide phragmoplast expansion during plant cytokinesis, Developmental Cell (2024), https://doi.org/10.1016/j.devcel.2024.05.015

CellPress

cortex during mitotic cell division in plants. To test this hypothesis, we captured the dynamics of a mitotically active Myosin XI motor and discovered its microtubule-coupled function in cytokinesis. Our findings identified a long-sought-after mechanism that regulates the determination of cell division planes in plant cells.

RESULTS

The Myosin XI motor MYA1/Myo11F marks the CDS and plays a role in division plane orientation

In *A. thaliana*, four of the 13 Myosin XI genes, namely *Myosin XI-1/MYA1*/Myo11F, *Myosin XI-2/MYA2/Myo11B2*, *Myosin XI-I/Myo11G*, and *Myosin XI-K/Myo11E*, have elevated expression in vegetative tissues.[11,13] The corresponding quadruple mutant (MyoXI-4KO hereafter) shows significant reduction in growth when compared with wild-type plants or mutants of lower orders.[14] Because F-actin plays a role in microtubule organization in both the PPB at prophase and the spindle midzone at early stages of cytokinesis,[12,15] we tested whether this MyoXI-4KO mutant experienced deficiencies in microtubule-associated activities. To do so, we grew seedlings on medium supplemented with 150 nM oryzalin (a microtubule-disrupting herbicide). The MyoXI-4KO mutant seedlings showed exacerbated growth defects in the presence of oryzalin, as evidenced by shorter roots when compared with the wild-type control, although the mutant and control roots did not grow significantly differently when exposed to the solvent DMSO alone (Figures 1A and S1A). To verify the linkage of this oryzalin-hypersensitive phenotype to the mutations in the myosin genes, we transformed the MyoXI-4KO mutant with a construct for MYA1/Myo11F expression with a GFP (green fluorescent protein) fusion under the control of the *MYA1/Myo11F* promoter. *MYA1/Myo11F* was chosen because of its high expression level in vegetative tissues.[13] The growth phenotype of the MyoXI-4KO mutant was suppressed by MYA1-GFP expression as the transgenic line, referred hereafter as "rescue," was comparable to the wild-type control (Figures 1A and S1A), confirming that the *mya1* mutation had a causative relationship with oryzalin hypersensitivity.

Oryzalin hypersensitivity could be due to cell division defects and/or defects in cell elongation due to the essential role of microtubules in cellulose deposition. Because the MyoXI-4KO mutant suffers severe defects in organelle movement, cytoplasmic streaming, and cell elongation already,[14] we cannot rule out the possibility of compromised cell expansion by oryzalin treatment. We chose to focus on the detected phenotype of cell division plane orientation in the myosin mutants in this study. First, the compromised root growth phenotype prompted us to examine whether MYA1 participated in cell division. In a transgenic line expressing MYA1-GFP and mCherry-TUB6 (β-tubulin 6), MYA1 exhibited a cell-cycle-dependent pattern of dynamic localization corresponding to the reorganization of mitotic microtubule arrays (Figure 1B; Video S1). At prophase, when the mature PPB was present (asterisks, Figure 1B), MYA1-GFP did not exhibit a discernable localization pattern at a specific site. At later stages of prophase, when the bipolar microtubule array establishes on the nuclear envelope and the PPB begins to be disassembled, MYA1-GFP becomes enriched in the cortical position occupied by the mature PPB (arrows, Figure 1B), which is defined as the cortical division zone (CDZ) at this stage.[5] This conspicuous localization of MYA1-GFP at the PPB site persisted throughout mitosis, until the expanding phragmoplast contacted it (asterisks, Figure 1B). MYA1-GFP was also enriched in the midzone of the metaphase spindle by highlighting microtubule bundles there (00:06:10, Figure 1B). The signal appeared more striking in the midzone of the developing phragmoplast, while persisting at the CDS as prominent foci (00:24:40, Figure 1B). Although the phragmoplast could be tilted at early stages of cytokinesis as shown, the associated MYA1 signal in its midzone eventually unified with that at both sides of the cortex when the microtubule array arrived there (arrowheads, 00:46:52, 01:20:23, Figure 1B). Therefore, the phragmoplast is actively guided toward the cortical position marked by MYA1-GFP.

(A) The Myosin XI quadruple mutant (MyoXI-4KO) displays hypersensitivity to oryzalin. Seedlings of wild-type (1), MyoXI-4KO (2), and MyoXI-4KO expressing MYA1-GFP (3) were grown on media without and with 150 nM oryzalin, which causes severe inhibition of root growth when compared with the wild-type control and the line expressing the MYA1-GFP transgene (rescue). Quantitative analysis of root length is shown in Figure S1A.

(B) MYA1 exhibits a cell-cycle-dependent localization pattern. MYA1-GFP localizes to the CDS at late prophase and continuously marks the CDS until the phragmoplast reaches the site. Cell cycle stages are marked as Pro (prophase), Meta (metaphase), and Cyto (cytokinesis). Asterisks point at the PPB and the positions after PPB disassembly. Arrows point at the cortical MYA1 signal when it first became detectable. Arrowheads indicate the unification of the phragmoplast MYA1 signal and that at the CDS.

(C) STED microscopy reveals the relationship between phragmoplast microtubules and MYA1-GFP, detected by dual immunostaining against tubulin and GFP. In the lateral view, MYA1 localizes to the cortex and in the midline of the phragmoplast. MYA1 forms a ring of discrete foci along the cell cortex in the axial view. Enlarged view (zoom) has phragmoplast microtubules contact the MYA1 foci.

(D) Three-dimensional (3D) projection of a living cell undergoing cytokinesis with MYA1-GFP (green) and microtubules (magenta), showing MYA1-GFP forming discrete foci along the cortex of the cell as well as localizing to the phragmoplast midzone.

(E) Immunolocalization of MYA1-GFP (pseudo-colored in green) and microtubules (magenta) in fixed cells with DNA (cyan) stained during each stage of cell division. Cells are viewed from two orientations, as illustrated in the micrograph. In the lateral view, MYA1 localizes to the cortex at prophase, remains at the PPB-defined site throughout cytokinesis, and is detected in the spindle and phragmoplast midzone. The axial view demonstrates the progression of cortical foci formation, starting from a diffuse ring at prophase to discrete foci by anaphase and cytokinesis.

(F) The MyoXI-4KO mutant forms misoriented cell plates when challenged by 150 nM oryzalin. Root cells of wild-type (1), MyoXI-4KO (2), and MyoXI-4KO expressing MYA1-GFP or rescue line (3) are outlined by propidium iodide staining. The mutant cells (2), but not the control or rescued ones, produce extensive misoriented cell plates in cells marked by asterisks. The degree of misorientation is also reported quantitatively in Figure S1B.

(G) The MyoXI-4KO mutant loses the expansion guidance of the cell plate marked by GFP-SYP111 upon oryzalin treatment. A root cell forms a tilted SYP111-labeled cell plate (green), which seeks maximum expansion in the diagonal direction (arrows). Following the expression of the MYA1-TagRFP fusion protein (magenta), the expanding cell plate marked by GFP-SYP111 (green) aims to unify with the CDS marked by MYA1-TagRFP.

See also Videos S1 and S4.

Please cite this article in press as: Huang et al., The microtubular preprophase band recruits Myosin XI to the cortical division site to guide phragmoplast expansion during plant cytokinesis, Developmental Cell (2024), https://doi.org/10.1016/j.devcel.2024.05.015

To determine how low doses of oryzalin compromised root growth in the MyoXI-4KO mutant, we examined mitotic microtubule arrays by live-cell imaging after having a visGreen-TUB6 expressed (Figure S1B; Videos S2 and S3). Although the mutant cells produced mitotic microtubule arrays similar to those of the complemented cells, as revealed by the mCherry-TUB6 fusion protein, they suffered severe challenges in establishing robust bipolar spindle microtubule arrays upon oryzalin treatment (−00:11:05 to 00:27:04, Figure S1B). Although the PPB array was detected and did not show noticeable difference to that in the control and rescue lines (arrowheads, −00:11:05, Figure S1B), very little if any microtubules were detected on the nuclear envelope at all stages of prophase. Then, conspicuous microtubules were assembled in the cell center and organized into flattened patterns that were hardly recognized as bipolar arrays (00:25:34 to 00:27:04, Figure S1B). The phragmoplast array formed and expanded but was turned 90° perpendicular to the PPB-defined plane (00:34:35 to 00:45:52, Figure S1B). Although the mitotic cell in the rescue line showed a similar delay in completing cell division, its spindle microtubule array was able to recover and reestablish bipolarity, resembling those in cells treated with DMSO, prior to anaphase onset (00:22:21). When the frequencies of these oryzalin-caused spindle defects were quantified in wild-type, MyoXI-4KO, and rescue plants, greater than 60% of the MyoXI-4KO cells showed the phenotype of collapsed spindle array while fewer than 40% of wild-type or rescue plant cells exhibited such transient defects (Figure S1C). Furthermore, the rescue cell showed no obvious defects in phragmoplast guidance. We conclude that the loss of the four Myosin XI motors caused serious defects in phragmoplast guidance as well as in the assembly of the bipolar spindle microtubule array, which became hypersensitive to the mild depolymerization challenges of microtubules.

To capture the relationship between MYA1/Myo11F and the developing phragmoplast microtubule array, we performed immunofluorescence experiments coupled with stimulated emission depletion (STED) microscopy in isolated root cells to improve the signal-to-noise ratio. Isolated cells were mounted on a microscope slide in different orientations, so that the cortex signal could be revealed in either lateral or axial planes in greater detail (Figure 1C). In a lateral view, parallel to the cell division axis, MYA1 was detected at the CDS (arrows) besides being enriched in the phragmoplast midzone (Figure 1C), reinforcing the live-cell-imaging results. Cells that were placed with the cell division axis perpendicular to the glass slide permitted us to take an axial view across the cell cortex. In this informative view, MYA1 was revealed to form a ring of discrete foci across the cell cortex (Figure 1C). Intriguingly, microtubules emanating from the leading edge of the phragmoplast often pointed toward these MYA1 foci, with the possibility of a connection (zoom image, arrowheads). These discrete cortical foci were also observed in living cells (Figure 1D), informing us that the immunostaining procedure preserved the subcellular localization of MYA1. We then asked at what stage of cell division these foci formed. MYA1 gradually accumulate in the PPB at the cortex in prophase, as informed by the fusiform prophase spindle microtubule array. The relatively uniform cortical signal at the CDS transitioned to foci by metaphase and became more conspicuous by anaphase. When phragmoplast expansion started in cytokinesis, MYA1 was clearly detected as discrete foci forming an intermittent ring at the cell cortex (Figure 1E). MYA1 localization at the CDS, and its conspicuous association with phragmoplast microtubules, supported a function of Myosin XI motors in the spatial regulation of cytokinesis in *A. thaliana*.

We then tested whether the oryzalin-hypersensitive growth defects were brought about by cytokinetic defects. When root cells were outlined by the fluorescence dye propidium iodide, the oryzalin-treated MyoXI-4KO root cells often formed randomly oriented cell plates (asterisks, Figure 1F). Meanwhile, the wild-type control and the rescue line produced cells with uniform orientations in each cell layer under identical conditions (Figure 1F). Quantifications of cell wall angles showed that, upon oryzalin treatment, the MyoXI-4KO root formed misoriented cell walls at random angles that frequently deviated from the typical 90° to the intercepting wall (Figure S1B). To determine how the mutant cells produced such misaligned cell plates, we had the MyoXI-4KO mutant express a GFP fusion of the syntaxin protein SYP111/KNOLLE, which served as a marker of the developing cell plate.[16] Upon oryzalin treatment, the MyoXI-4KO mutant cell formed the cell plate that sought to expand diagonally (arrows, Figure 1G; Video S4). This cytokinetic defect was suppressed in mutants expressing a functional MYA1-TagRFP fusion protein that marked the CDS, as cells formed the regular, transverse cell plate parallel to others in the same cell layer (arrowheads) (Video S4). This result suggested that the MyoXI-4KO mutant cells failed to form cell plates perpendicularly oriented to the cell division axis. Furthermore, MYA1 precisely marked the cell plate fusion site where the cell plate fused with the mother cell wall. In combination with MYA1 localization and the MyoXI-4KO cell plate misalignment, we concluded that MYA1 is a CDS protein that controlled the orientation of the cell division plane by guiding phragmoplast expansion during cytokinesis.

Formation of the cytoskeleton-associated motor assemblies at the PPB site (CAMP)

Like MYA1, a few other proteins have been detected at the CDS throughout late stages of mitotic cell division in *A. thaliana*, including the Ran GTPase-activating protein1 (RanGAP1), the microtubule-based motor proteins POK1/2, and the microtubule-associated proteins TAN1 and MAP65-4.[17–20] Furthermore, Myosin XI-K/Myo11E also was detected at the CDS.[9] To examine the relationship between MYA1/Myo11F and these previously reported CDS-localized proteins, we performed dual-localization experiments in root meristematic cells isolated from plants co-transformed with constructs expressing MYA1 and proteins of interest, which were tagged with their respective fluorescent protein or the complementary 4xMyc or PA tags. At the lateral view, the MYA1 signal overlapped with those of all five CDS proteins—Myosin XI-K, RanGAP1, TAN1, POK1, and MAP65-4 (Figures 2A–2D and S2). Because these foci occupied the cortex in an intermittent ring, the axial view allowed us to examine these proteins across the entire perimeter at the cortex. All five CDS proteins formed discrete cortical foci that colocalized with the MYA1 foci (Figures 2A–2D and S2). To further reveal the spatial relationship between MYA1 and these established CDS proteins in the axial view, fluorescence intensity scans of the CDS-localized signals were performed to graphically capture

Please cite this article in press as: Huang et al., The microtubular preprophase band recruits Myosin XI to the cortical division site to guide phragmoplast expansion during plant cytokinesis, Developmental Cell (2024), https://doi.org/10.1016/j.devcel.2024.05.015

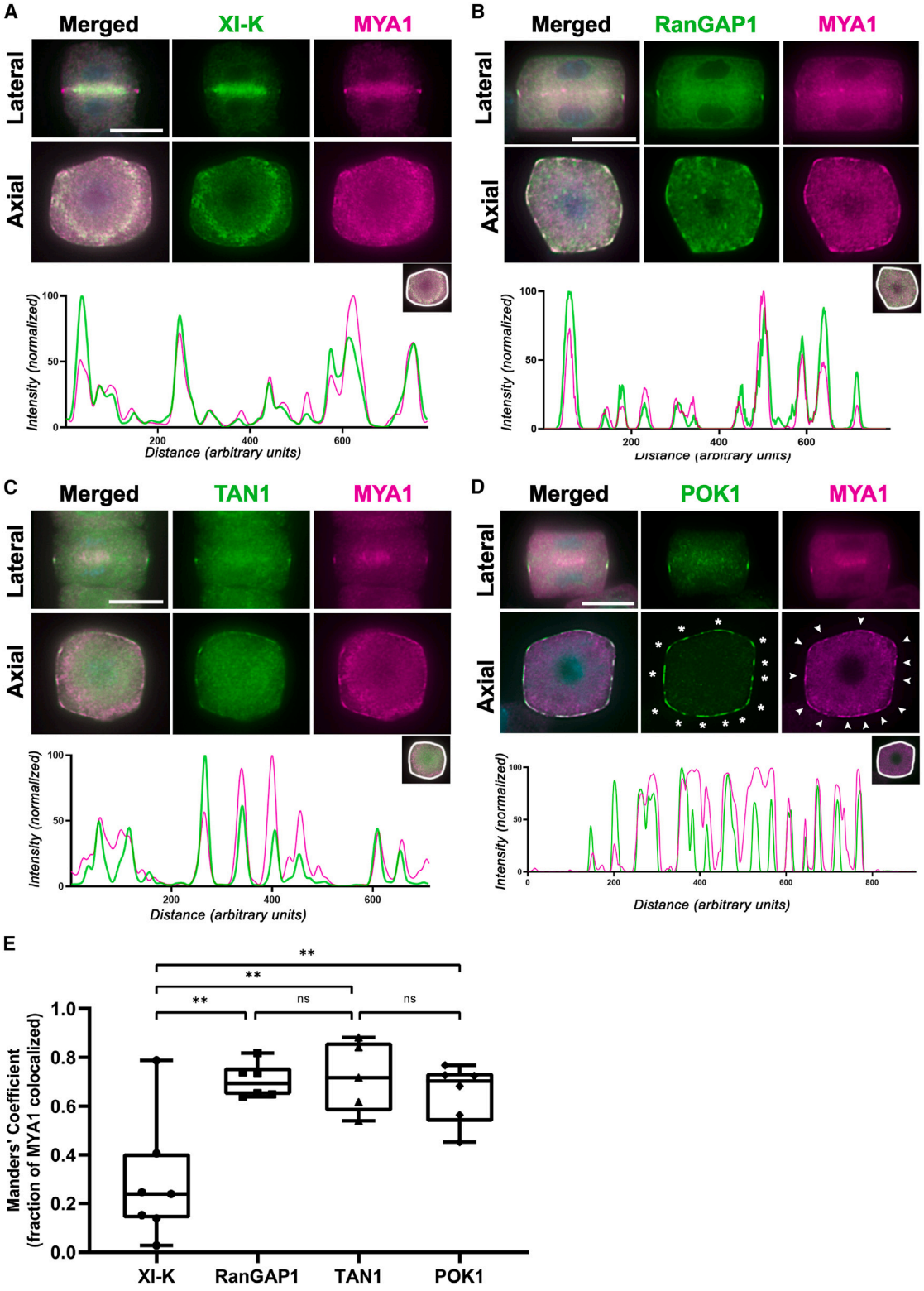

Figure 2. Myosin XI and other CDS cytoskeletal proteins form discrete foci of the cytoskeleton-associated motor assemblies at PPB site (CAMP) *in vivo*

Scale bars: 5 μm.

(A–D) MYA1 colocalizes with other CDS proteins in cortical foci. Micrographs show dual localizations of MYA1-4xMyc (pseudo-colored in magenta) and Myosin XI-K-YFP (green) (A), MYA1-4xMyc (magenta) and RanGAP1-PA (green) (B), MYA1-GFP (magenta) and TAN1-4xMyc (green) (C), and MYA1-4xMyc (magenta)

(legend continued on next page)

Please cite this article in press as: Huang et al., The microtubular preprophase band recruits Myosin XI to the cortical division site to guide phragmoplast expansion during plant cytokinesis, Developmental Cell (2024), https://doi.org/10.1016/j.devcel.2024.05.015

colocalizations in the form of overlapping peaks. Such colocalization patterns were quantified by comparing Manders' colocalization coefficients between the MYA1/Myo11F signal overlapping with that of either Myosin XI-K, RanGAP1, TAN1, or POK1, respectively, at the cell cortex in the axial view (Figure 2E). Because MYA1 almost completely colocalizes with RanGAP1, TAN1, and POK1 along the cortex, the Manders' coefficient was greater than 0.7. However, the Myosin XI-K/Myo11E signal at the cell cortex was weaker and sometimes not obvious when compared with that of MYA1/Myo11F, reflected by the lower colocalization coefficient (Figure 2E). It is worth noting that MYA1, Myosin XI-K, RanGAP1, and MAP65-4 were clearly detected at both the CDS and in the phragmoplast midzone, whereas TAN1 and POK1 were conspicuous at the CDS but not obviously noticeable in the phragmoplast midzone, similar to what has been reported previously.[7,18,20] This phenomenon suggests that perhaps different assemblies of cytoskeletal factors are formed in the phragmoplast and at the CDS. Our results demonstrated the colocalization of MYA1/Myo11F with known CDS proteins in the cortical foci. Therefore, we concluded that at least MYA1/Myo11F, Myosin XI-K/Myo11E, RanGAP1, TAN1, POK1, and MAP65-4 assembled into discrete cytoskeletal foci at the CDS established by the PPB, which were termed cytoskeleton-associated motor assemblies at the PPB site (CAMP), reflecting the formation of high-order molecular assemblies.

To test whether the Myosin XI motors described above physically associated with each other *in vivo*, we performed anti-GFP immunoprecipitation experiments using transgenic plants co-expressing Myosin XI-K-YFP and MYA1-4xMyc. The bait of XI-K-YFP fusion protein was detected on replicate membrane blots containing identical protein samples by the anti-GFP antibodies as well as polyclonal antibodies raised against a myosin XI-K specific peptide (arrowheads, Figure S3A). The precipitates also included the MYA1-4xMyc fusion protein, which was revealed by a polyclonal anti-cMyc antibody (Figure S3A). These myosin fusion proteins were specifically isolated because they were absent when similar anti-GFP immunoprecipitation experiments were performed using extracts of plants expressing GFP alone (Figure S3B). To test whether the association of two myosins was dependent on intact F-actin or their motility on the track, we had truncated MYA1$^{874–1,520}$-GFP and Myosin XI-K$^{881–1,531}$-4xMyc fusion proteins, lacking the motor and the IQ domains, expressed in tobacco leaf cells. When MYA1$^{874–1,520}$-GFP was captured by anti-GFP immuno-affinity purification, as detected by the anti-GFP antibody by immune-blotting, Myosin XI-K$^{881–1,531}$-4xMyc was also detected by both the anti-Myosin XI-K and anti-cMyc antibodies (Figure S3C). When the motorless truncation of the kinesin ATK5, ATK51$^{–390}$-GFP, was co-expressed with Myosin XI-K$^{881–1,531}$-4xMyc and captured by the anti-GFP beads, the later was not detected (Figure S3D). Therefore, we concluded that the two actin motors were able to physically associate with each other *in vivo*.

The striking colocalization of MYA1 with the established CDS proteins inspired us to test whether CAMPs were a result of physical association. To do so, we performed an anti-GFP immunoprecipitation experiment using plants expressing YFP-POK1.[21] POK1 was chosen due to its elevated expression in mitotic cells as well as being primarily localized at the CDS, making it the candidate of choice to dissect protein association in CAMPs. We were able to detect by mass spectrometry the bait protein POK1 in three biological replicates (Figure 3A). Together with POK1, MYA1 and RanGAP1 were consistently co-purified together (Figure 3A). In addition, Myosin XI-K as well as TAN1 and pleckstrin homology GAP1 (PHGAP1 or RhoGAP with PH domain) were detected. Both PHGAP1 and RanGAP1 are CDS proteins and directly interact with POK1.[19,21] Plants expressing free GFP served as a negative control. Proteins detected at the CAMP were specifically co-purified with POK1 but were not detected when GFP was purified under identical conditions (Figure 3A). As a further validation of protein-protein association, TAN1 and MYA1 colocalization within the CAMP foci were resolve by using STED super-resolution microscopy. We observed that some CAMP proteins display intriguing localization patterns within foci defined by MYA1. Three representative CAMP proteins, RanGAP1, TAN1, and POK1, formed sub-foci within a larger MYA1 focus (asterisks, Figures 3B–3D). Taken together, our results here further supported the notion that the CAMP harbored, but is not limited to, Myosin XI and Kinesin-12 motors together with other cytoskeleton-associated factors like TAN1, RanGAP1, and PHGAP1.

Formation of the CAMP at the CDS requires the PPB and the POK1/2 kinesins

Because MYA1 localized to the PPB site and consequently was detected at the CDS at later stages of mitotic division, we asked how the disturbance of PPB assembly would affect MYA1 localization. Three functionally redundant microtubule-associated proteins TRM6, TRM7, and TRM8 (TON1 recruiting motifs 6, 7, and 8) play critical roles in the assembly of the PPB microtubule array as the *trm678* triple mutant exhibits various degrees of PPB defects.[22] We examined MYA1 localization in the *trm678* triple mutant cells and found that the MYA1 signal was still detectable at the CDS, although it often appeared only at one side of the cell in a lateral view of the dividing cells, while its localization in the phragmoplast midzone was still conspicuous (Figure 4A). Such a phenomenon prompted us to examine cells from an axial view. In the *trm678* mutant, isolated, sparse MYA1 foci were found in the cell perimeter representing the CDS at the focal plane (Figure 4A). To verify that the abnormal distribution of MYA1 foci was caused by the loss of the TRM function, we employed a complemented line in which TRM7-3xYFP and

and YFP-POK1 (green) (D) from lateral and axial views. The accompanying graphs on the bottom are results of fluorescence intensity scans of the two respective signals in the highlighted peripheral line encompassing the CAMP by using the merged images (inserts). The fluorescence intensities are normalized, with the brightest signal set at 100 and the x axis with the cell perimeters set in arbitrary units.

(E) Manders' colocalization coefficient of the cortical MYA1 signal overlapping with those of Myosin XI-K, RanGAP1, TAN1, and POK1, respectively. Only signals in the axial view are compared in each pair. Myosin XI-K has the lowest coefficient. In contrast, RanGAP1, TAN1, and POK1 overlapped well with MYA1, resulting in a high coefficient. The comparisons have $\geq$5 cells for each dual localization. The difference is determined significant based on a two-tailed t test with a p value < 0.01 (**).

Please cite this article in press as: Huang et al., The microtubular preprophase band recruits Myosin XI to the cortical division site to guide phragmoplast expansion during plant cytokinesis, Developmental Cell (2024), https://doi.org/10.1016/j.devcel.2024.05.015

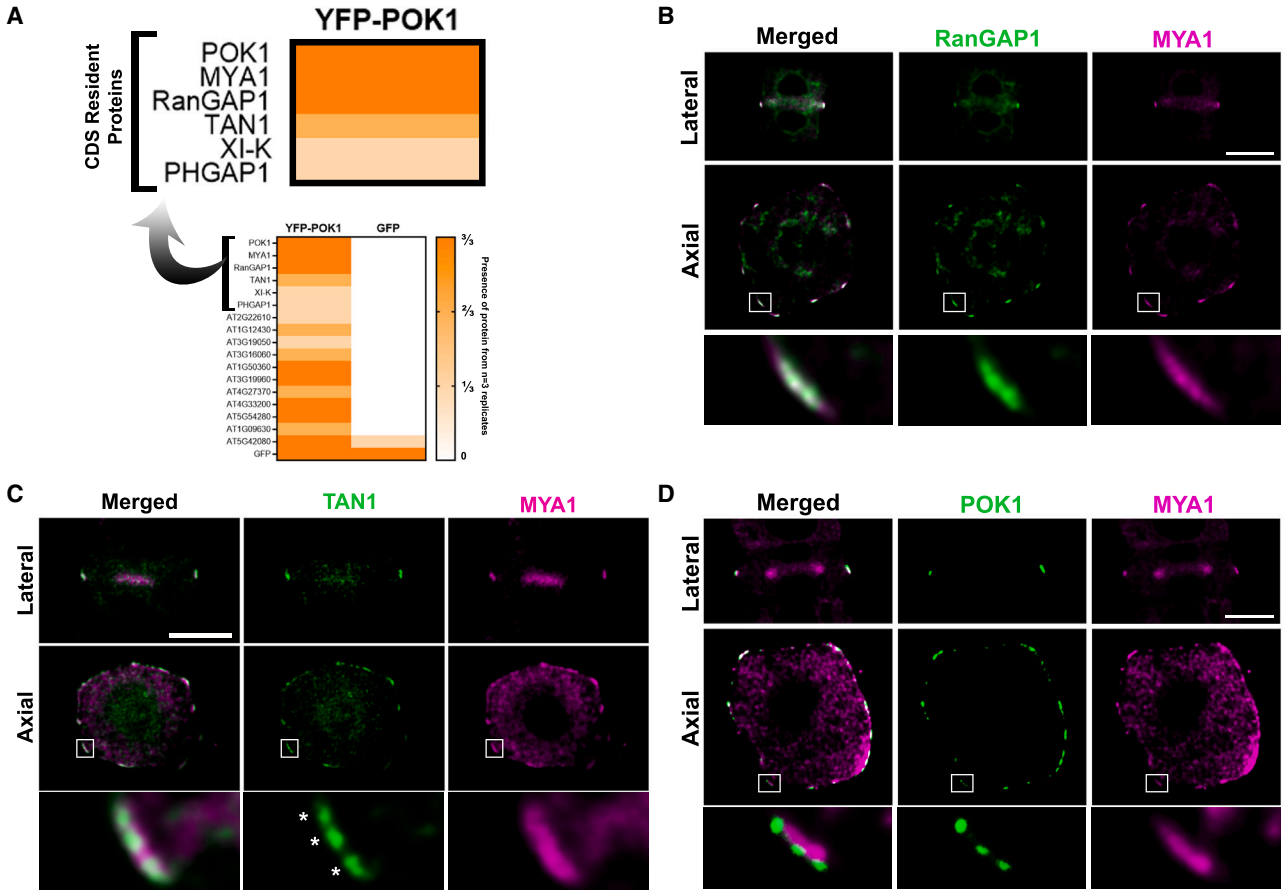

Figure 3. Co-purification and colocalization of the CAMP proteins

(A) Immunoaffinity purification of YFP-POK1 reveals the association of MYA1, Myosin XI-K, RanGAP1, TAN1, and PHGAP1 *in vivo*. The identification and enrichment of these CDS-resident proteins was performed using Gene Ontology (GO) terms for cytoskeleton-related activities. The heatmap qualitatively shows the presence of these proteins out of three biological replicates. A similar purification aimed at free GFP is used as a reference for the determination of the specificity of detected proteins. All proteins identified by mass spectrometry are shown in Table S1.

(B–D) The localization of RanGAP1, TAN1, POK1, and MYA1 is re-examined using STED microscopy. Both lateral and axial views are shown. In the lateral view, RanGAP1, TAN1, and POK1 colocalize with MYA1 along the cell cortex. In the axial view, RanGAP1, TAN1, and POK1 foci are shown to consist of smaller punctae within the MYA1 foci (enlarged image). Scale bars, 5 μm.

See also Table S1.

MYA1-4xMyc were expressed in the *trm678* triple mutant. In this rescue line, the cortical MYA1 localization pattern was restored in distinct foci (Figure 4A). As a control for our quantifications, we examined MYA1 foci in the rescue line expressing MYA1-GFP, which developed normal PPB (asterisks, Figure 4A). The arrangement of MYA1 foci became irregularly distanced from each other in the *trm678* mutant. The distances between adjacent foci were measured using the cell perimeter as a reference. Although the rescue cells had distances approximately 9% of the perimeter (9.256% ± 0.554%), the *trm678* mutant cells' distances were more than doubled, at approximately 20% of the perimeter on average (20.201% ± 1.83%) (Figure 4B). Therefore, the results suggested that defects of PPB assembly affected the formation of the otherwise regularly spaced MYA1 foci at the CDS in the *trm678* mutant. This phenotype of irregular MYA1 foci in the *trm678* mutant echoed its increased variance in division planes, as reported previously.[22] Using this complemented/rescue line expressing TRM7-3xYFP, we observed localizations of TRM7 and MYA1in metaphase cells because TRM7 is no longer detectable at the CDS by anaphase.[22] Both proteins were detected at the CDS in the lateral view (Figure 4C). The axial view showed that the remnant TRM7 signal was detected across the CDS, while the MYA1 cortical foci were clearly formed by metaphase across the cell perimeter (Figure 4C). It is worth noting that TRM7 displays a more continuous localization across the cell cortex in the axial view, while MYA1 shows discrete peaks, as represented by fluorescence intensity scans across the cell cortex (Figure 4C). To take one step further, we then asked whether the PPB was essential for MYA1 to assume the localization at the CDS by employing the *fass* mutant that fails to establish the PPB at the cell cortex.[23] When MYA1-GFP was expressed in the *fass* mutant cells, it was clearly detected in the phragmoplast but became undetectable at the cell cortex in both lateral and axial views (Figure 4D). Taken together, it became clear that not only patterning of foci were altered in these PPB defective mutants but also the number of foci. To

Please cite this article in press as: Huang et al., The microtubular preprophase band recruits Myosin XI to the cortical division site to guide phragmoplast expansion during plant cytokinesis, Developmental Cell (2024), https://doi.org/10.1016/j.devcel.2024.05.015

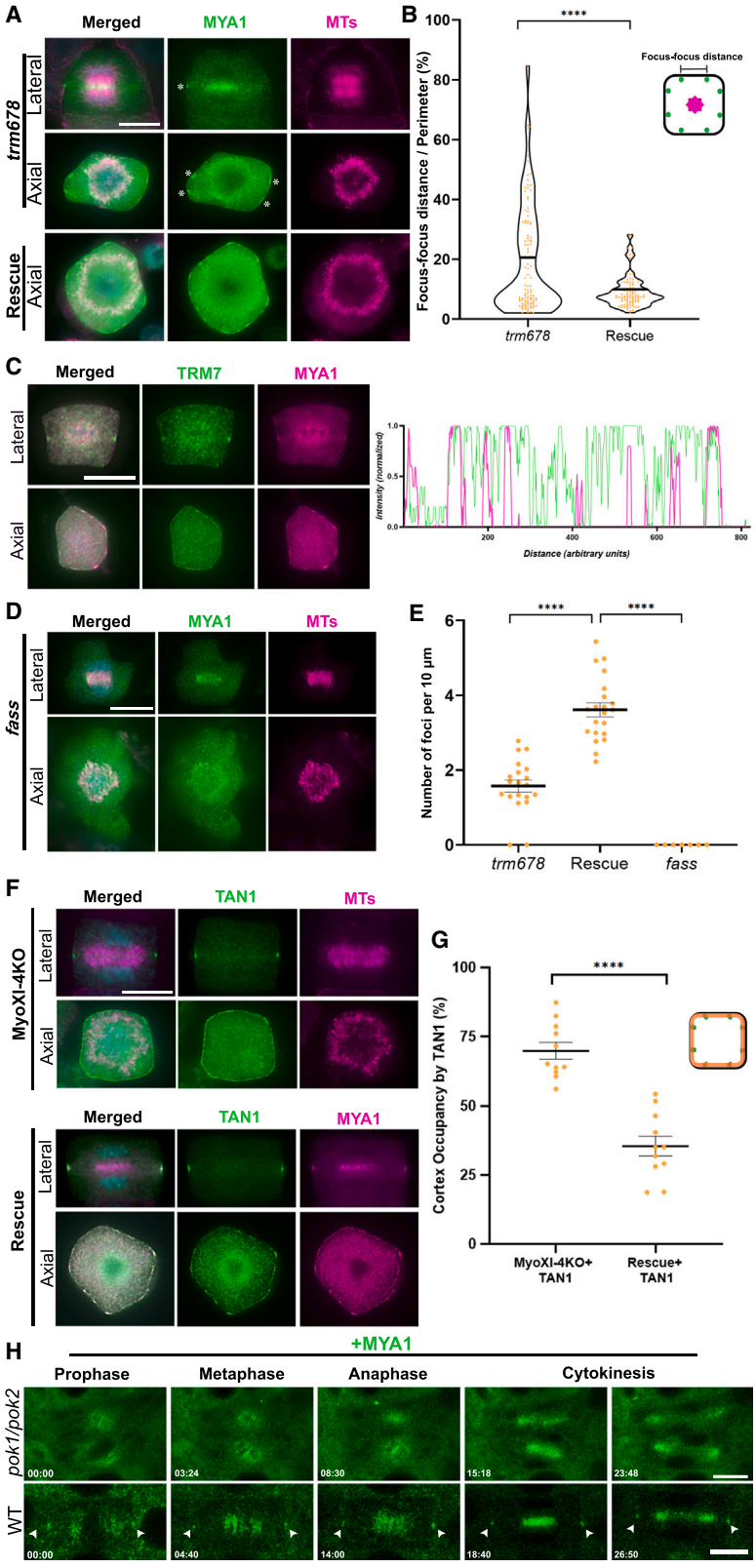

Figure 4. MYA1 localization and CAMP formation at the cortex are dependent on the PPB

Scale bars: 5 μm in (C), (F), and (H).

(A) MYA1 localization at the CDS is disrupted in the *trm678* mutant cells. When examined from the lateral view, the MYA1 (pseudo-colored in green) signal often stands out only at one side of the mutant cell (asterisk), while its presence in the midzone of phragmoplast microtubule (MT) array (magenta) remains conspicuous. An axial view shows sparse, irregularly distanced MYA1 foci at the cell cortex (asterisks). The pattern of regularly distanced MYA1 foci is restored in cells expressing TRM proteins (rescue).

(B) The patterns of MYA1 foci in the *trm678* mutant and rescue line are assessed in the form of the distance between adjacent foci. Greater than 90 foci are measured in more than 10 cells of each genotype. The difference is determined significant based on a two-tailed t test with a p value < 0.0001 (****). Means are marked by a solid black line.

(C) TRM and MYA1 show different localization patterns at the CDZ/CDS. Both TRM7-3xYFP (pseudo-colored in green) and MYA1-4xMyc fusion protein (magenta) are detected at the CDS from the lateral view. Although MYA1 is detected in discrete foci from the axial view, remnants of the TRM7 signal remain at the cortex across the cell perimeter. Signal intensity along the cell cortex is displayed graphically, showing discrete and well-separated peaks for MYA1 and continuous TRM7 signal in wide regions. (D) MYA1 no longer forms cortical foci in the *fass* mutant lacking the PPB. Although MYA1 (green) can be detected in the association with phragmoplast microtubules (magenta) in both lateral and axial views, no discernable signal stands above the background at the cell cortex.

(E) The numbers of MYA1 foci are determined in the *trm678*, *fass* mutants, and the rescue line, and are presented quantitatively per 10 μm. Sample sizes are $n = 7$ cells for *fass*, and $n \geq 20$ cells for *trm678* and rescue lines. The difference is determined significant based on a two-tailed t test with a p value < 0.0001 (****).

(F) TAN1 localization at the cell cortex is altered in the MyoXI-4KO mutant. Although TAN1-4xMyc (pseudo-colored in green) is detected at the CDS, as shown in the lateral view, it becomes nearly continuous across the CDS from the axial view. In the rescued MyoXI-4KO plant expressing MYA1-GFP (magenta) and TAN1-4xMyc (green), however, discrete foci are detected in the axial view.

(G) The distribution of TAN1 signal is quantified by the percentage occupancy of TAN1 across the cell cortex underneath the plasma membrane in the axial view. The MyoXI-4KO mutant cells have diffuse TAN1 signal, therefore occupying more of the cortex, while cells of the rescued plant have TAN1 more enriched in foci, which occupies less of the cortex. Cortex occupancy was measured from $n \geq 10$ cells per genotype. The difference is determined significant based on a two-tailed t test with a p value < 0.0001 (****).

(H) MYA1-3xCitrine localization in wild-type (WT) and *pok1/pok2* mutant cells. MYA1 foci accumulate at the cortex as the WT cell progresses into mitosis and cytokinesis (arrowheads). The cortical MYA1 localization is no longer noticeable in the *pok1/pok2* mutants. However, MYA1 is still conspicuously detected in the spindle and phragmoplast midzones in the mutant cells. MYA1-3xCitrine is pseudo-colored in green. See also Video S5.

Please cite this article in press as: Huang et al., The microtubular preprophase band recruits Myosin XI to the cortical division site to guide phragmoplast expansion during plant cytokinesis, Developmental Cell (2024), https://doi.org/10.1016/j.devcel.2024.05.015

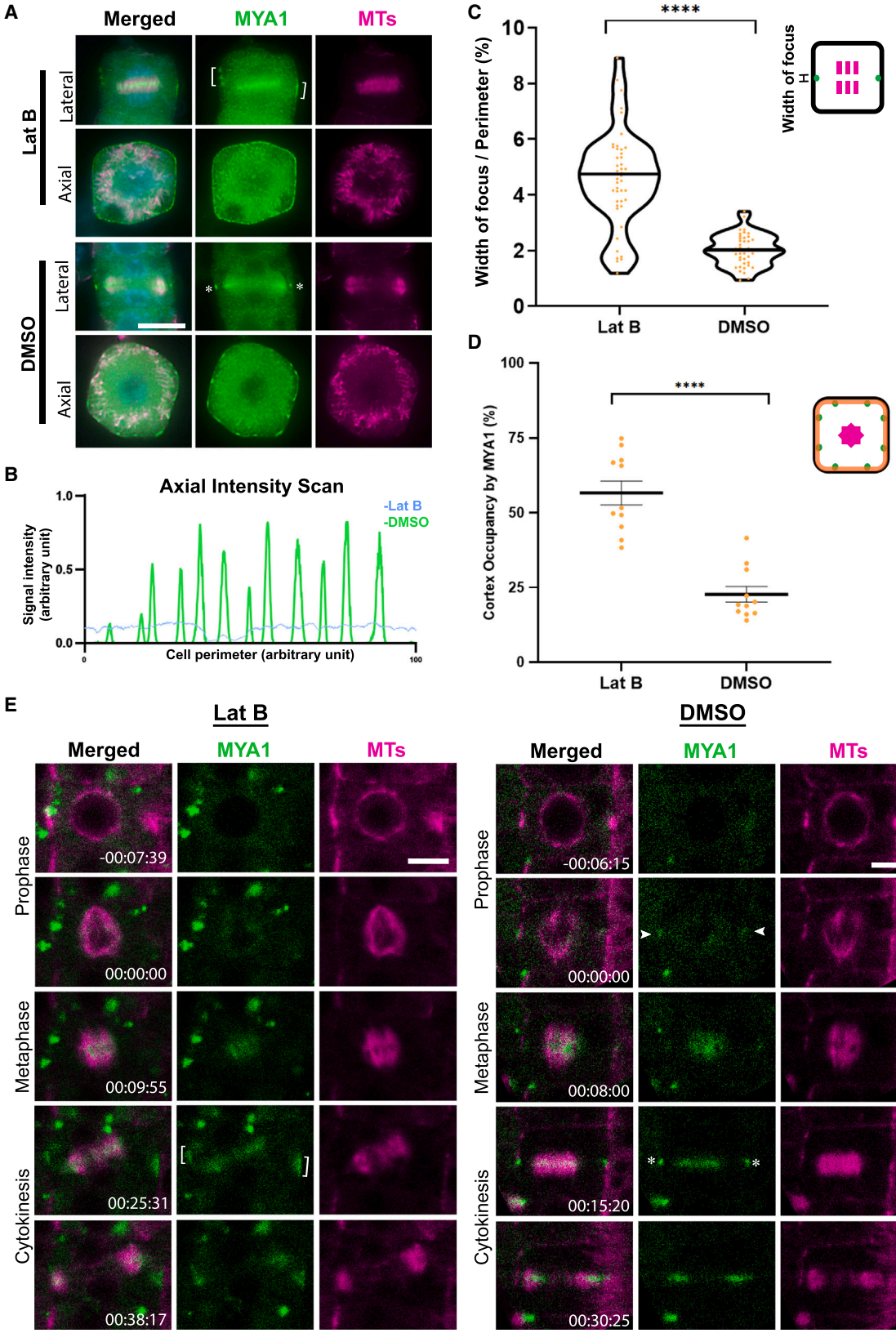

(legend on next page)

Please cite this article in press as: Huang et al., The microtubular preprophase band recruits Myosin XI to the cortical division site to guide phragmoplast expansion during plant cytokinesis, Developmental Cell (2024), https://doi.org/10.1016/j.devcel.2024.05.015

report this difference in MYA1 foci among the *trm678* and *fass* mutants as well as the TRM7-3xYFP rescue line, we quantified the number of MYA1 foci per 10 μm of the cell perimeter. The number dropped significantly, to an average of 1–2 (1.573 ± 0.161) foci/10 μm in the *trm678* mutant and to 0 in the *fass* mutant, while the rescue cell formed 3–4 (3.614 ± 0.186) foci/10 μm (Figure 4E). These results led to the conclusion that the PPB is required for MYA1 localization at the CDS. Coincidentally, it is known that TAN1 recruitment to the CDS is lost in the *ton2* mutant.[18] In the less-severe *trm678* mutant, POK1 localization to the CDS is affected, although not completely abolished.[22] Conversely, we asked whether the formation of the CAMP might be affected in the MyoXI-4KO mutant. TAN1 was used as a marker of CAMP and was still detected at the CDS in both lateral and axial views in the MyoXI-4KO mutant (Figure 4F). In the axial view, however, the discrete TAN1 foci were replaced by nearly continuous signal across the perimeter in the MyoXI-4KO mutant cells. The rescued plants expressing a functional MYA1 fusion protein had the TAN1 signal return to discrete foci (Figure 4F). This observation was quantified by measuring the percentage of the cortex that is occupied by the TAN1 signal (Figure 3F). In the MyoXI-4KO background, the continuous TAN1 signal occupied about 70% of the cortex perimeter (69.88% ± 3.03%). When rescued by a functional MYA1 fusion protein, the TAN1 foci had lower occupancy of the cortex, at about 35% (35.4% ± 3.6%). Similarly, when POK1 localization was examined in the MyoXI-4KO mutant, the kinesin still decorated the CDS, but in a more uniform fashion (Figure S4A). Taken together, these results led to the conclusion that the PPB was required for the initial localization of CAMP proteins to the CDS, and the Myosin XI motors played a role in organizing these CDS-localized proteins into discrete CAMPs appearing in foci, although it was not required for the initial localization.

Because the functionally redundant Kinesin-12 motors POK1 and POK2 are required for TAN1 maintenance at the CDS after PPB disassembly,[20] we then asked whether the kinesins also regulated Myosin XI at the cortex. To do so, the MYA1-3xCitrine fusion protein was expressed in the *pok1/pok2* double mutant background. In the control cells with the wild-type background, MYA1 accumulated in the spindle and phragmoplast midzones and was detected at the CDS when they progressed into mitosis and cytokinesis (arrowheads, Figure 4H; Video S5). In the *pok1/pok2* double mutant cells, however, MYA1 was no longer conspicuously at the CDS but still accumulated in the spindle and phragmoplast midzones (Figure 4H). Taken together, these results led to the conclusions that both PPB and POK1/2 are required for the localization of the CAMP proteins at the CDS and that Myosin XI played a critical role in organizing these CDS-localized proteins into discrete CAMP foci. These results also serve as evidence for physical association between Kinesin-12 and Myosin XI during cell division in *A. thaliana*.

F-actin plays a critical role in the formation of phragmoplast-recognizable CAMPs

F-actin exhibits a dynamic reorganization pattern at the cell cortex during mitosis, first colocalizing with the PPB and later disappearing from the mature PPB and remaining largely absent at the PPB-defined CDS for much of the later mitotic stages.[4,24] Because F-actin functions as myosin tracks and plays an essential role in cell division plane orientation, we first tested whether the F-actin localization pattern was changed during cytokinesis in the MyoXI-4KO mutant. To do so, we carried out anti-actin immunofluorescence experiments and found that F-actin filaments inside the phragmoplast and cell cortex were similar in cells of MyoXI-4KO, the wild-type, and the mutant expressing MYA1-GFP (Figure S4B). This result prompted us to ask whether the CAMP formation and MYA1 localization were dependent on the intact F-actin network. When F-actin was depolymerized by latrunculin B (Lat B), the MYA1 signal was dispersed vertically in the cell division axis at the cell cortex, compared with the consolidated MYA1 signal at the CDS in the mock/DMSO-treated cells (Figure 5A). To examine whether the signal diffusion only took place along

Figure 5. Consolidation of the CAMP requires intact F-actin

All micrographs have MYA1 pseudo-colored in green and microtubules in magenta. Scale bars: 5 μm.

(A) Latrunculin B (Lat B) treatment causes diffusion of the MYA1 signal at the CDS. MYA1 appears in expanded zones (brackets) following the treatment when the cell is examined from a lateral view, although its appearance in the phragmoplast midzone remains concentrated. From an axial view, MYA1 loses its appearance in discrete foci, which are replaced by nearly continuous signal across the perimeter. Mock-treated cells exhibit normal localization patterns of MYA1 in consolidated foci at the CDS. The micrographs have MYA1 pseudo-colored in green, microtubules (MTs) in magenta, and DNA in cyan in the merged images.

(B) Assessment of MYA1-GFP signal distribution across the cell perimeter between Lat B and DMSO treatment. The fluorescent signal intensity is reported in arbitrary units, using the sum of the MYA1-GFP signal as the reference. The x axis represents the linearized cell perimeter in arbitrary units from the starting point (0) to finishing point (100).

(C) Quantitative assessment of the width of the MYA1 foci shows significant expansion along the division axis. The occupation of the cell cortex/perimeter by the width of a MYA1 focus is determined in the lateral view and reported in percentages. Each treatment has the sample size $n > 40$ cells. The difference in MYA1 signal occupancy of the cell perimeter (in percentage) between mock and Lat B-treated cells is determined significant, using a two-tailed t test with a p value < 0.0001 (****). Means are marked by solid black lines.

(D) The percentage occupancy of MYA1 signal along the cortex at the axial axis is measured to quantify the effects of Lat B on MYA1 along the cortex. In Lat B-treated cells, the MYA1 signal becomes diffuse along the cortex, which occupies more of the cortex. In DMSO/mock-treated cells, MYA1 foci are formed in discrete regions, occupying less of the cortex. Cortex occupancy is measured from $n \geq 10$ cells per treatment. The difference is determined significant based on a two-tailed t test with a p value < 0.0001 (****).

(E) Lat B treatment causes diffusion of MYA1 at the CDS in transgenic cells expressing both MYA1-GFP (green) and mCherry-TUB6 (magenta). In a mitotic cell treated with Lat B, the MYA1 signal is readily detected at the cell cortex in a diffuse form (brackets) when the phragmoplast is formed. In a mock (DMSO)-treated cell, MYA1 is detected at the CDS as consolidated signals (asterisks). In the meantime, MYA1 localization in the phragmoplasts after both Lat B and DMSO treatments does not show noticeable differences by live-cell imaging. The merged images have MYA1-GFP pseudo-colored in green, microtubules (MTs) in magenta.

See also Video S6.

Please cite this article in press as: Huang et al., The microtubular preprophase band recruits Myosin XI to the cortical division site to guide phragmoplast expansion during plant cytokinesis, Developmental Cell (2024), https://doi.org/10.1016/j.devcel.2024.05.015

CellPress

the division axis, the cells were also examined from an axial view. We found that the discrete MYA1 foci were replaced by nearly continuous signal across the cell perimeter after Lat B treatment (Figure 5A). An intensity scan of the MYA1 fluorescent signal across the perimeter in the axial view demonstrated the peaks and troughs reflecting the foci formed in the DMSO-treated cell, whereas the Lat B-treated cell displayed a close-to-linear intensity pattern due to the diffuse signal (Figure 5B). To further assess the vertical diffusion of the MYA1 signal, we measured the width of the MYA1 signal in the lateral view by using the total perimeter of the cell in this same focal plane as a reference. In the Lat B-treated cells, the MYA1 signal occupied greater than 4.5% of the perimeter (4.583% ± 0.2578%) compared with having the signal confined within approximately 2% of the cell perimeter (2.02% ± 0.087%) in the mock-treated cells—a difference of more than 2-fold dispersal (Figure 5C). To quantify the diffuse MYA1 signal shown in the axial view, we measured the percentage of cortex occupancy with and without Lat B treatment. Lat B caused MYA1 foci to become diffuse, therefore occupying about approximately 57% (56.59% ± 3.97%) of the cortex perimeter. MYA1 foci were formed normally in the DMSO treatment, which occupied less than 23% (22.71% ± 2.62%) of the perimeter (Figure 5D). Because CAMPs consist of different cytoskeletal proteins, including TAN1 and the Kinesin-12 POK1, which show progressive localization patterns from diffuse broad bands at metaphase to discontinuous foci during cytokinesis,[18,20] we asked whether POK1 also required F-actin to be concentrated in discrete cortical foci by co-expressing both YFP-POK1 and MYA1-4xMyc. Like MYA1, the CDS-localized POK1 requires F-actin to become concentrated in the lateral view and consolidated into discrete foci shown in the axial view (Figures S4C and S4D). The results led to the conclusion that intact F-actin filaments were essential for the consolidation of CAMPs in both lateral and axial axes. Finally, we asked whether the actin-dependent CAMP formation was coupled with division plane determination by employing cells expressing both MYA1-GFP and mCherry-TUB6 to monitor myosin localization, with microtubule arrays as references (Video S6). After Lat B treatment, MYA1 was detected in the spindle midzone (−00:07:39 to 00:09:55, Figure 5E). Following mitosis, the developing phragmoplast became tilted while the diffuse MYA1 signal was detected at the cell cortex (brackets, 00:25:31, Figure 5E). Toward the end of cytokinesis, the phragmoplast microtubule array and the associated MYA1 signal remained tilted, irrespective of the orientation of the CDS-localized, diffuse MYA1 signal (00:38:17, Figure 5E). In the mock-treated cells, in contrast, the MYA1-GFP signal became concentrated at the CDS around the time of NEB (00:00:00, arrowheads, Figure 5E). The CDS-localized MYA1 signal persisted at later stages of mitosis and became most conspicuous around the time when the phragmoplast microtubule array was expanding centrifugally (asterisks, 00:15:20, Figure 5E). Concomitantly with the expanding microtubule array, the phragmoplast-localized MYA1 signal was always aligned with the MYA1-marked CDS, and eventually merged with the cortical signal (00:30:25, Figure 5E). We concluded that the diffuse cortical MYA1 signal caused by Lat B was no longer recognizable by the developing phragmoplast.

DISCUSSION

Our results showed PPB-dependent recruitment of Myosin XI to the CDS, where it was incorporated into macromolecular assemblies containing the Kinesin-12 motor and other microtubule-associated proteins, as well as RanGAP1.

Formation of cytoskeletal motor assemblies at the CDZ/CDS

The PPB is formed in a PP2A-complex-dependent manner and defines the CDZ/CDS during somatic mitotic divisions.[23,25] Published studies led to the model of PPB-guided recruitment of the TAN1, POK1, and RanGAP proteins to the CDZ, where they are anchored to guide the expanding phragmoplast toward the cell plate fusions site.[6] During cytokinesis, TAN1 stabilizes cortical-telophase microtubules and POK1 captures microtubules emanating from the phragmoplast edge so that the two populations of microtubules are incorporated prior to having the cell plate fused at its fusion site.[20,26] Here, we integrate the contribution of myosin XI motors to division plane determination to the existing models, with an emphasis of high-order cytoskeletal assemblies of both microtubule- and F-actin-associated factors at the CDS (Figure 6). Early, broad PPB microtubule arrays recruit microtubule-associated proteins like TAN1, MAP65-4, and then the kinesin POK1 to bridge and engage neighboring microtubules.[7] Following the maturation or condensation of the PPB microtubule array, probably brought about by MAP65 via its microtubule-bundling activities along with an unknown F-actin-dependent function,[12] the PPB brings in important additional cytokinesis factors like RanGAP1 and Myosin XI motors (Figure 6). Emanating from the phragmoplast edge,[20] microtubules recognized these CAMP foci at the cortex so that the expansion became guided. Our results suggested that microtubules extending from the leading edge of the phragmoplast might be captured by kinesin(s) like POK1 and/or other MAPs such as TAN1 present in these CAMPs. In fact, a recent report demonstrated microtubule plus-end capture and pausing when microtubules contact TAN1.[26] Although it is unclear how CAMP proteins may pull the microtubules at the phragmoplast edge to ultimately anchor the phragmoplast, our results provide the evidence of a direct connection between phragmoplast microtubules and the CDS via proteins that directly interact with microtubules and F-actin.

Association of myosin XI and kinesin-12 for cell division

We were intrigued by how the seemingly separated Myosin XI and Kinesin-12 motors are physically associated with each other. There have been a few published cases of kinesin-myosin association *in vivo*. For example, the budding yeast Myosin V Myo2 and kinesin SMY1 physically associate with each other through direct interaction and play a synergistic role in vesicle delivery/docking to the bud tip.[27] So, how were the functionally coupled Myosin XI and Kinesin-12 motors brought together physically at the CDZ/CDS? The abundant recovery of the RanGAP proteins with POK1 invited us to hypothesize that the protein might play a moonlighting role in forming the CAMP besides its function in nucleocytoplasmic trafficking. A mitotic role of RanGAP has also been detected in mammalian cells, although on spindle microtubules and kinetochores.[28] In *A. thaliana*, RanGAP1 serves as a permanent marker at the CDS in mitotic

Please cite this article in press as: Huang et al., The microtubular preprophase band recruits Myosin XI to the cortical division site to guide phragmoplast expansion during plant cytokinesis, Developmental Cell (2024), https://doi.org/10.1016/j.devcel.2024.05.015

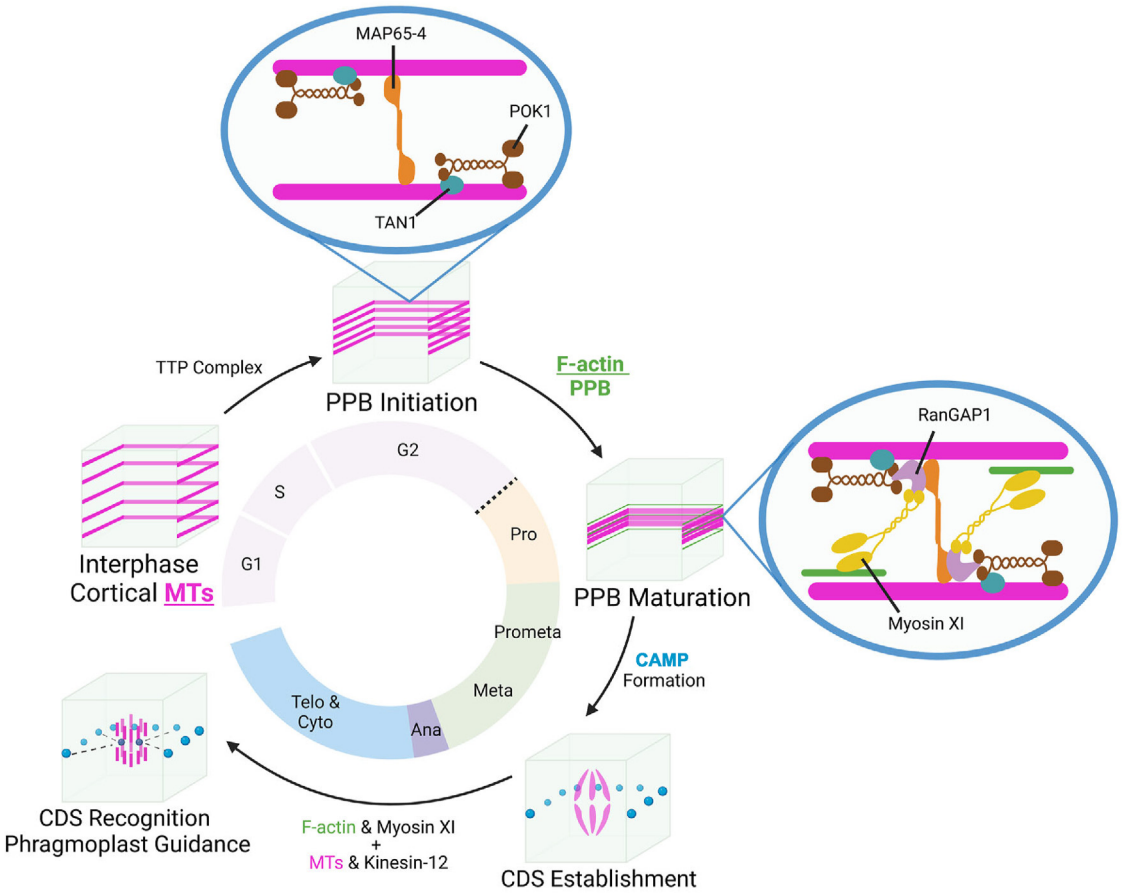

Figure 6. Schematic presentation of CAMP formation and phragmoplast guidance during mitotic division in somatic plant cells

Following the TTP (TON1-TRM-PP2A)-complex-dependent induction of PPB formation, microtubule-associated factors like MAP65-4 and TAN1, together with its associated POK1 kinesin, are recruited to the wide PPB. Narrow PPB establishes the CDZ and attracts RanGAP1 and Myosin XI to existing microtubule-interacting factors. F-actin in the PPB allows Myosin XI to consolidate these cytoskeletal factors into CAMPs, which are devoted to guiding the expanding phragmoplast toward the cell plate fusion site during cytokinesis. CAMPs persist at the CDS at later stages of mitosis until the phragmoplast midzone-localized MYA1 and other proteins unify with those in the CAMP to allow the expanding cell plate to insert into this PPB-defined site toward the end of cytokinesis.

root cells and, together with functionally redundant RanGAP2, is essential—at least in part—for cell division.[19] How RanGAP regulates division plane orientation, as suggested by the phenotype of disorganized cell files in the *RanGAP* knockdown mutant in *A. thaliana*,[29] is largely unknown. Further dissection of the structure and function of RanGAP may bring insights into its relationship with myosin and kinesin motors during cytokinesis.

We are excited to learn that the function of Myosin XI was integrated with that of POK1 at the CDS. Previously, Myosin VIII was detected at microtubule plus-ends in the expanding phragmoplast and was hypothesized to bridge the interaction between phragmoplast microtubules and actin filaments nucleated from the CDS.[6,8] Together with the earlier detection of Myosin XI-K/Myo 11E at the CDS,[9] our results prompted us to hypothesize that the actin-based motor Myosin XI perhaps was responsible for organizing the POK1 motor into macromolecular complexes, seen here as the CAMP, as the function requires intact actin filaments. Such a function may be expressed more prominently in certain cells, such as the subsidiary mother cell in maize in which the loss of the Myosin XI motor OPAQUE1 (O1) leads to misguidance of phragmoplast expansion.[30] Our results indicated that the cortical localization of Myosin XI was abolished in the *pok1 pok2* double mutant. Together with the importance of the intact F-actin network, we demonstrated that POK1/2 function in the recruitment of Myosin XI, which likely acts on F-actin to drive the formation of the CAMP foci.

It is worth noting that such kinesin-myosin association may be applied to the spindle and phragmoplast midzone as well. This notion is in part supported by the detection of MYA1/Myo11F inside spindles and phragmoplasts, which was independent of F-actin. In addition, studies in tobacco cells revealed an F-actin function in microtubule organization in the central spindle at late anaphase and telophase.[15] The detection of the moss Myosin XI inside mitotic spindles also supported the notion that such a possible function of myosin XI in mitosis may be shared—at least among land plants.[31] Our results showed that POK1/2 were not required for MYA1/Myo11F localization to the spindle and phragmoplast midzones. Therefore, other microtubule-associated factors, perhaps Kinesin-12A/B that function exclusively in the midzones,[32,33] may interact with myosin XI motors for phragmoplast localization. Again, such actin-microtubule interaction may be equally important for plant cytokinesis.

Please cite this article in press as: Huang et al., The microtubular preprophase band recruits Myosin XI to the cortical division site to guide phragmoplast expansion during plant cytokinesis, Developmental Cell (2024), https://doi.org/10.1016/j.devcel.2024.05.015

In summary, the CAMP, assembled by Myosin XI, Kinesin-12, and other microtubule-associated proteins, as well as RanGAP1 at the CDS, are recognized by the expanding phragmoplast to allow the developing cell plate to be inserted at the site defined by the PPB. This study, therefore, inspires us to investigate how proteins of different cytoskeletal elements congregate to form dynamic CAMPs for spatial regulation of cytokinesis in land plants.

Limitations of the study

Although this study demonstrated the important association of Myosin XI and Kinesin-12 motors for division plane orientation, it did not reveal how the motor activities contributed to the process.

STAR★METHODS

Detailed methods are provided in the online version of this paper and include the following:

- KEY RESOURCES TABLE
- RESOURCE AVAILABILITY
  - Lead contact
  - Materials availability
  - Data and code availability
- EXPERIMENTAL MODEL AND STUDY PARTICIPANT DETAILS
- METHOD DETAILS
  - Arabidopsis Mutants and Growth Tests
  - Plasmid Construction and Expression in *Plants*
  - Immunoprecipitation and Immunoblotting Analysis
  - Analysis of co-purified proteins from mass spectrometry
  - Indirect Immunofluorescence and Confocal Microscopy
  - Analysis of Root Growth and Plane of Division
  - Quantification of Collapsed Spindles
  - Analysis of Cortical Foci
- QUANTIFICATION AND STATISTICAL ANALYSIS

SUPPLEMENTAL INFORMATION

Supplemental information can be found online at https://doi.org/10.1016/j.devcel.2024.05.015.

ACKNOWLEDGMENTS

This work was supported by NSF grants 1920358 and 2148207, and the United States Department of Agriculture (USDA) —the National Institute of Food and Agriculture (NIFA) under an Agricultural Experiment Station (AES) hatch project (CA-D-PLB-2536-H). We are indebted to Dr. Valerian V. Dolja for sharing the myosin XI constructs and seeds, Dr. David Bouchez and Dr. Martine Pastuglia for the *trm*, *ton*, and *fass* lines, Dr. Sabine Müller for the YFP-POK1 and *pok1/2* lines, Dr. Masa H. Sato for the GFP-*SYP111* plasmid, Dr. Iris Meier for RanGAP lines, and Dr. Tsuyoshi Nakagawa for the pGWB plasmids. We want to thank Dr. John Harada for examining the manuscript and his critical comments.

AUTHOR CONTRIBUTIONS

C.H.H., F.L.P., Y.-R.J.L., and B.L. conceptualized the project and designed experiments. C.H.H., F.L.P., and Y.-R.J.L. performed the experiments. All authors participated in data analysis. C.H.H. and B.L. wrote the original draft of the manuscript, with inputs from other authors. All authors edited the manuscript.

DECLARATION OF INTERESTS

The authors declare no competing interests.

Received: June 16, 2023
Revised: February 22, 2024
Accepted: May 14, 2024
Published: June 6, 2024

REFERENCES

1. Gunning, B.E.S. (1982). The cytokinetic apparatus: its development and spatial regulation. In The Cytoskeleton in Plant Growth and Development, C.W. Lloyd, ed. (Academic Press), pp. 230–288.
2. Facette, M.R., Rasmussen, C.G., and Van Norman, J.M. (2019). A plane choice: coordinating timing and orientation of cell division during plant development. Curr. Opin. Plant Biol. *47*, 47–55. https://doi.org/10.1016/j.pbi.2018.09.001.
3. Palevitz, B.A., and Hepler, P.K. (1974). Control of Plane of Division during Stomatal Differentiation in Allium. 2. Drug Studies. Chromosoma *46*, 327–341. https://doi.org/10.1007/BF00284885.
4. Liu, B., and Palevitz, B.A. (1992). Organization of cortical microfilaments in dividing root cells. Cell Motil. Cytoskel *23*, 252–264. https://doi.org/10.1002/cm.970230405.
5. Smertenko, A., Assaad, F., Baluška, F., Bezanilla, M., Buschmann, H., Drakakaki, G., Hauser, M.T., Janson, M., Mineyuki, Y., Moore, I., et al. (2017). Plant Cytokinesis: Terminology for Structures and Processes. Trends Cell Biol. *27*, 885–894. https://doi.org/10.1016/j.tcb.2017.08.008.
6. Livanos, P., and Müller, S. (2019). Division Plane Establishment and Cytokinesis. Annu. Rev. Plant Biol. *70*, 239–267. https://doi.org/10.1146/annurev-arplant-050718-100444.
7. Mills, A.M., Morris, V.H., and Rasmussen, C.G. (2022). The localization of PHRAGMOPLAST ORIENTING KINESIN1 at the division site depends on the microtubule-binding proteins TANGLED1 and AUXIN-INDUCED IN ROOT CULTURES9 in Arabidopsis. Plant Cell *34*, 4583–4599. https://doi.org/10.1093/plcell/koac266.
8. Wu, S.Z., and Bezanilla, M. (2014). Myosin VIII associates with microtubule ends and together with actin plays a role in guiding plant cell division. eLife *3*, e03498. https://doi.org/10.7554/eLife.03498.
9. Abu-Abied, M., Belausov, E., Hagay, S., Peremyslov, V., Dolja, V., and Sadot, E. (2018). Myosin XI-K is involved in root organogenesis, polar auxin transport, and cell division. J. Exp. Bot. *69*, 2869–2881. https://doi.org/10.1093/jxb/ery112.
10. Tominaga, M., and Nakano, A. (2012). Plant-specific myosin XI, a molecular perspective. Front. Plant Sci. *3*, 211. https://doi.org/10.3389/fpls.2012.00211.
11. Madison, S.L., and Nebenführ, A. (2013). Understanding myosin functions in plants: are we there yet? Curr. Opin. Plant Biol. *16*, 710–717. https://doi.org/10.1016/j.pbi.2013.10.004.
12. Mineyuki, Y., and Palevitz, B.A. (1990). Relationship between preprophase band organization F actin and the division site in *Allium* fluorescence and morphometric studies on cytochalasin-treated cells. J. Cell Sci. *97*, 283–295. https://doi.org/10.1242/jcs.97.2.283.
13. Okamoto, K., Ueda, H., Shimada, T., Tamura, K., Kato, T., Tasaka, M., Morita, M.T., and Hara-Nishimura, I. (2015). Regulation of organ straightening and plant posture by an actin-myosin XI cytoskeleton. Nat. Plants *1*, 15031. https://doi.org/10.1038/nplants.2015.31.
14. Peremyslov, V.V., Prokhnevsky, A.I., and Dolja, V.V. (2010). Class XI myosins are required for development, cell expansion, and F-Actin organization in Arabidopsis. Plant Cell *22*, 1883–1897. https://doi.org/10.1105/tpc.110.076315.
15. Maeda, K., Sasabe, M., Hanamata, S., Machida, Y., Hasezawa, S., and Higaki, T. (2020). Actin Filament Disruption Alters Phragmoplast Microtubule Dynamics during the Initial Phase of Plant Cytokinesis. Plant Cell Physiol. *61*, 445–456. https://doi.org/10.1093/pcp/pcaa003.
16. Enami, K., Ichikawa, M., Uemura, T., Kutsuna, N., Hasezawa, S., Nakagawa, T., Nakano, A., and Sato, M.H. (2009). Differential expression control and polarized distribution of plasma membrane-resident SYP1

Please cite this article in press as: Huang et al., The microtubular preprophase band recruits Myosin XI to the cortical division site to guide phragmoplast expansion during plant cytokinesis, Developmental Cell (2024), https://doi.org/10.1016/j.devcel.2024.05.015

SNAREs in *Arabidopsis thaliana*. Plant Cell Physiol. *50*, 280–289. https://doi.org/10.1093/pcp/pcn197.

17. Li, H., Sun, B., Sasabe, M., Deng, X., Machida, Y., Lin, H., Lee, Y.R.J., and Liu, B. (2017). *Arabidopsis* MAP65-4 plays a role in phragmoplast microtubule organization and marks the cortical cell division site. New Phytol. *215*, 187–201. https://doi.org/10.1111/nph.14532.
18. Walker, K.L., Müller, S., Moss, D., Ehrhardt, D.W., and Smith, L.G. (2007). Arabidopsis TANGLED identifies the division plane throughout mitosis and cytokinesis. Curr. Biol. *17*, 1827–1836. https://doi.org/10.1016/j.cub.2007.09.063.
19. Xu, X.M., Zhao, Q., Rodrigo-Peiris, T., Brkljacic, J., He, C.S., Müller, S., and Meier, I. (2008). RanGAP1 is a continuous marker of the Arabidopsis cell division plane. Proc. Natl. Acad. Sci. USA *105*, 18637–18642. https://doi.org/10.1073/pnas.0806157105.
20. Lipka, E., Gadeyne, A., Stöckle, D., Zimmermann, S., De Jaeger, G., Ehrhardt, D.W., Kirik, V., Van Damme, D., and Müller, S. (2014). The phragmoplast-orienting Kinesin-12 class proteins translate the positional Information of the preprophase band to establish the cortical division zone in *Arabidopsis thaliana*. Plant Cell *26*, 2617–2632. https://doi.org/10.1105/tpc.114.124933.
21. Stöckle, D., Herrmann, A., Lipka, E., Lauster, T., Gavidia, R., Zimmermann, S., and Müller, S. (2016). Putative RopGAPs impact division plane selection and interact with kinesin-12 POK1. Nat. Plants *2*, 16120. https://doi.org/10.1038/nplants.2016.120.
22. Schaefer, E., Belcram, K., Uyttewaal, M., Duroc, Y., Goussot, M., Legland, D., Laruelle, E., de Tauzia-Moreau, M.L., Pastuglia, M., and Bouchez, D. (2017). The preprophase band of microtubules controls the robustness of division orientation in plants. Science *356*, 186–189. https://doi.org/10.1126/science.aal3016.
23. Spinner, L., Gadeyne, A., Belcram, K., Goussot, M., Moison, M., Duroc, Y., Eeckhout, D., De Winne, N., Schaefer, E., Van De Slijke, E., et al. (2013). A protein phosphatase 2A complex spatially controls plant cell division. Nat. Commun. *4*, 1863. https://doi.org/10.1038/ncomms2831.
24. Rasmussen, C.G., Wright, A.J., and Müller, S. (2013). The role of the cytoskeleton and associated proteins in determination of the plant cell division plane. Plant J. *75*, 258–269. https://doi.org/10.1111/tpj.12177.
25. Drevensek, S., Goussot, M., Duroc, Y., Christodoulidou, A., Steyaert, S., Schaefer, E., Duvernois, E., Grandjean, O., Vantard, M., Bouchez, D., and Pastuglia, M. (2012). The Arabidopsis TRM1-TON1 interaction reveals a recruitment network common to plant cortical microtubule arrays and eukaryotic centrosomes. Plant Cell *24*, 178–191. https://doi.org/10.1105/tpc.111.089748.
26. Bellinger, M.A., Uyehara, A.N., Allsman, L., Martinez, P., McCarthy, M.C., and Rasmussen, C.G. (2023). Cortical microtubules contribute to division plane positioning during telophase in maize. Plant Cell *35*, 1496–1512. https://doi.org/10.1093/plcell/koad033.
27. Beningo, K.A., Lillie, S.H., and Brown, S.S. (2000). The yeast kinesin-related protein Smy1p exerts its effects on the class V myosin Myo2p via a physical interaction. Mol. Biol. Cell *11*, 691–702. https://doi.org/10.1091/mbc.11.2.691.
28. Joseph, J., Tan, S.H., Karpova, T.S., McNally, J.G., and Dasso, M. (2002). SUMO-1 targets RanGAP1 to kinetochores and mitotic spindles. J. Cell Biol. *156*, 595–602. https://doi.org/10.1083/jcb.200110109.
29. Boruc, J., Griffis, A.H.N., Rodrigo-Peiris, T., Zhou, X., Tilford, B., Van Damme, D., and Meier, I. (2015). GAP Activity, but Not Subcellular Targeting, Is Required for Arabidopsis RanGAP Cellular and Developmental Functions. Plant Cell *27*, 1985–1998. https://doi.org/10.1105/tpc.114.135780.
30. Nan, Q., Liang, H., Mendoza, J., Liu, L., Fulzele, A., Wright, A., Bennett, E.J., Rasmussen, C.G., and Facette, M.R. (2023). The OPAQUE1/DISCORDIA2 myosin XI is required for phragmoplast guidance during asymmetric cell division in maize. Plant Cell *35*, 2678–2693. https://doi.org/10.1093/plcell/koad099.
31. Orr, R.G., Furt, F., Warner, E.L., Agar, E.M., Garbarino, J.M., Cabral, S.E., Dubuke, M.L., Butt, A.M., Munson, M., and Vidali, L. (2021). Rab-E and its interaction with myosin XI are essential for polarised cell growth. New Phytol. *229*, 1924–1936. https://doi.org/10.1111/nph.17023.
32. Lee, Y.R.J., Li, Y., and Liu, B. (2007). Two Arabidopsis phragmoplast-associated kinesins play a critical role in cytokinesis during male gametogenesis. Plant Cell *19*, 2595–2605. https://doi.org/10.1105/tpc.107.050716.
33. Müller, S., and Livanos, P. (2019). Plant Kinesin-12: localization heterogeneity and functional implications. Int. J. Mol. Sci. *20*, 4213. https://doi.org/10.3390/ijms20174213.
34. Nakagawa, T., Kurose, T., Hino, T., Tanaka, K., Kawamukai, M., Niwa, Y., Toyooka, K., Matsuoka, K., Jinbo, T., and Kimura, T. (2007). Development of series of gateway binary vectors, pGWBs, for realizing efficient construction of fusion genes for plant transformation. J. Biosci. Bioeng. *104*, 34–41. https://doi.org/10.1263/jbb.104.34.
35. Nakamura, S., Mano, S., Tanaka, Y., Ohnishi, M., Nakamori, C., Araki, M., Niwa, T., Nishimura, M., Kaminaka, H., Nakagawa, T., et al. (2010). Gateway binary vectors with the bialaphos resistance gene, bar, as a selection marker for plant transformation. Biosci. Biotechnol. Biochem. *74*, 1315–1319. https://doi.org/10.1271/bbb.100184.
36. Zhang, B.L., You, C.J., Zhang, Y., Zeng, L.P., Hu, J., Zhao, M.L., and Chen, X.M. (2020). Linking key steps of microRNA biogenesis by TREX-2 and the nuclear pore complex in Arabidopsis. Nat. Plants *6*, 957–969. https://doi.org/10.1038/s41477-020-0726-z.
37. Liu, W., Wang, C., Wang, G., Ma, Y., Tian, J., Yu, Y., Dong, L., and Kong, Z. (2019). Towards a better recording of microtubule cytoskeletal spatial organization and dynamics in plant cells. J. Integr. Plant Biol. *61*, 388–393. https://doi.org/10.1111/jipb.12721.
38. Kong, Z., Hotta, T., Lee, Y.R.J., Horio, T., and Liu, B. (2010). The γ-tubulin complex protein GCP4 is required for organizing functional microtubule arrays in Arabidopsis thaliana. Plant Cell *22*, 191–204. https://doi.org/10.1105/tpc.109.071191.
39. Silhavy, D., Molnár, A., Lucioli, A., Szittya, G., Hornyik, C., Tavazza, M., and Burgyán, J. (2002). A viral protein suppresses RNA silencing and binds silencing-generated, 21- to 25-nucleotide double-stranded RNAs. EMBO J. *21*, 3070–3080. https://doi.org/10.1093/emboj/cdf312.
40. Lee, Y.R.J., and Liu, B. (2000). Identification of a phragmoplast-associated kinesin-related protein in higher plants. Curr. Biol. *10*, 797–800. https://doi.org/10.1016/s0960-9822(00)00564-9.
41. Edelstein, A.D., Tsuchida, M.A., Amodaj, N., Pinkard, H., Vale, R.D., and Stuurman, N. (2014). Advanced methods of microscope control using μManager software. J. Biol. Methods *1*, e10. https://doi.org/10.14440/jbm.2014.36.
42. Bolte, S., and Cordelières, F.P. (2006). A guided tour into subcellular colocalization analysis in light microscopy. J. Microsc. *224*, 213–232. https://doi.org/10.1111/j.1365-2818.2006.01706.x.

Please cite this article in press as: Huang et al., The microtubular preprophase band recruits Myosin XI to the cortical division site to guide phragmoplast expansion during plant cytokinesis, Developmental Cell (2024), https://doi.org/10.1016/j.devcel.2024.05.015

CellPress

STAR★METHODS

KEY RESOURCES TABLE

REAGENT or RESOURCE	SOURCE	IDENTIFIER
Antibodies		
Rabbit polyclonal anti-GFP	ThermoFisher	A-6455
Mouse monoclonal anti-α-tubulin (DM1A)	Sigma	T9026
Donkey polyclonal anti-mouse Texas Red-conjugated	Rockland Immunochemicals	610-709-124
Donkey polyclonal anti-rabbit Fluorescein-conjugated	Rockland Immunochemicals	611-702-127
Goat polyclonal anti-rat Alexa Fluor 568-conjugated	ThermoFisher	A-11077
Goat polyclonal anti-rabbit Alexa Fluor 488-conjugated	ThermoFisher	A-11008
Mouse monoclonal anti-c-Myc	DSHB	AB_2266850
Rabbit polyclonal anti-c-Myc	Millipore Sigma	C3956-100UG
Sheep anti-tubulin	Cytoskeleton, Inc.	ATN02
Rat monoclonal anti-PA	FUJIFILM Wako Chemicals	016-25861
Donkey polyclonal anti-sheep Texas Red-conjugated	Rockland Immunochemicals	613-709-168
Goat anti-rabbit Antibody, HRP-conjugate	Millipore Sigma	SKU 12-348
Bacterial strains		
DH5α	ThermoFisher	18265017
GV3101	Gold Biotechnology	CC-105
Biological samples		
Arabidopsis- MyoXI-4KO	Peremyslov et al.[14]	N/A
Arabidopsis- trm678	Schaefer et al.[22]	N/A
Arabidopsis- fass-5	Spinner et al.[23]	N/A
Arabidopsis- pok1-1/pok2-3	Lipka et al.[20]	N/A
Arabidopsis- pok1-1/pok2-3 + proPOK1::YFP:POK1	Lipka et al.[20]	N/A
Arabidopsis- proSYP111::GFP:SYP111	Enami et al.[16]	N/A
Arabidopsis- MyoXI-4KO + proMYA1::MYA1:GFP	This paper	N/A
Arabidopsis- fass5 + proMYA1::MYA1:GFP	This paper	N/A
Arabidopsis- Myosin xi 3KO + proXIK::XIK:YFP + proMYA1::MYA1:4xMyc	This paper	N/A
Arabidopsis- pok1-1/pok2-3 + proMYA1:MYA1:3xCitrine	This paper	N/A
Arabidopsis- WT Col + proMYA1::MYA1:3xCitrine	This paper	N/A
Arabidopsis- trm678 + proMYA1::MYA1:GFP	This paper	N/A
Arabidopsis- rangap1-1/rangap2-3 + proRanGAP1::RanGAP1-PA + proMYA1:MYA1:4xMyc	This paper	N/A
Arabidopsis- trm678 + proTRM7::TRM7:3xYFP + proMYA1::MYA1:4xMyc	This paper	N/A
Arabidopsis- MyoXI-4KO + proTAN1::TAN1:3xCitrine	This paper	N/A
Arabidopsis- MyoXI-4KO + proMYA1::MYA1:GFP + proTUB6::mCherry:TUB6	This paper	N/A
Arabidopsis- MyoXI-4KO + proTUB6::mCherry:TUB6	This paper	N/A
Arabidopsis- MyoXI-4KO + proSYP111::GFP:SYP111	This paper	N/A
Arabidopsis- MyoXI-4KO + proSYP111::GFP:SYP111 + proMYA1::MYA1:TagRFP	This paper	N/A
Arabidopsis- pok1-1/pok2-3+ proPOK1::YFP:POK1 + proMYA1::MYA1:4xMyc	This paper	N/A
Arabidopsis- MyoXI-4KO + proTAN1::TAN1:3xCitrine + proMYA1::MYA1:4xMyc	This paper	N/A

(*Continued on next page*)

Please cite this article in press as: Huang et al., The microtubular preprophase band recruits Myosin XI to the cortical division site to guide phragmoplast expansion during plant cytokinesis, Developmental Cell (2024), https://doi.org/10.1016/j.devcel.2024.05.015

Continued

REAGENT or RESOURCE	SOURCE	IDENTIFIER
Arabidopsis- map65-4 + proMAP65-4::MAP65-4:GFP + proMYA1::MYA1:4xMyc	This paper	N/A
Chemicals, peptides, and recombinant proteins		
Cellulase RS	Yakult Pharmaceutical	Cellulase Onozuka™ RS
Murashige & Skoog Basal Salt Mix	MP Biomedicals	092623022
Phytagel	Sigma	P8169
Hygromycin B	A.G. Scientific	H-1012-PBS
BASTA, glufosinate ammonium	Bayer	04193473
3.5-Dinitro-N4. N4-dipropylsulfanilamide (Oryzalin)	Chemservice	N-12729
Latrunculin B	Millipore Sigma	428020
Propidium Iodide	ThermoFisher	BMS500PI
Dimethylsulfoxide (DMSO)	Millipore Sigma	D8418
SlowFade™ Diamond Antifade Mountant with DAPI	ThermoFisher	S36964
ProLong™ Glass Antifade Mountant	ThermoFisher	P36980
Paraformaldehyde	Electron Microscopy Sciences	15710
Restriction enzyme EcoRI	New England BioLabs	R0101S
Restriction enzyme MluI	New England BioLabs	R3198S
Restriction enzyme SalI	New England BioLabs	R0138S
Restriction enzyme NotI	New England BioLabs	R0189S
Restriction enzyme NcoI	New England BioLabs	R3193S
Restriction enzyme EcoRV	New England BioLabs	R3195S
Restriction enzyme KpnI	New England BioLabs	R3142S
Restriction enzyme XhoI	New England BioLabs	R0146S
Critical commercial assays		
μMACS Anti-GFP Isolation Kit	Miltenyi Biotec	130-091-125
Trans-Blot Turbo RTA Mini 0.2 μm PVDF Transfer Kit	Bio-Rad	1704272
Clarity™ Western ECL Substrate	Bio-Rad	1705060
Phusion Hot Start II DNA Polymerase	ThermoFisher	F549S
Gateway LR Clonase II Enzyme mix	ThermoFisher	11791020
Gibson Assembly Master mix	New England BioLabs	E2611
pENTR/D-TOPO cloning kit	ThermoFisher	K240020
Experimental models: Organisms/strains		
Arabidopsis thaliana	ABRC	CS1092
Oligonucleotides		
In Table S2	N/A	N/A
Recombinant DNA		
pGWB1	Nakagawa et al.[34]	N/A
pGWB4	Nakagawa et al.[34]	N/A
pGWB16	Nakagawa et al.[34]	N/A
pGWB616	Nakamura et al.[35]	N/A
pGWB559	Nakamura et al.[35]	N/A
pGWB6023	Zhang et al.[36]	N/A
pMpGWB123	Addgene	68577
pENTR4	ThermoFisher	A10465
pCH1	This paper	N/A
pGEX-4T2	Addgene	27458101
Myosin XI-K cDNA	NCBI	NM_001343671
MYA1 cDNA	NCBI	NM_101620
ATK5 cDNA	NCBI	NM_116758

(*Continued on next page*)

Please cite this article in press as: Huang et al., The microtubular preprophase band recruits Myosin XI to the cortical division site to guide phragmoplast expansion during plant cytokinesis, Developmental Cell (2024), https://doi.org/10.1016/j.devcel.2024.05.015

Continued

REAGENT or RESOURCE	SOURCE	IDENTIFIER
Software and algorithms		
ImageJ	NIH	N/A
Huygens Professional	Huygens Software Suite	N/A
ZEN Black	Carl Zeiss	N/A
Leica Application Suite X	Leica	N/A
Metamorph	Molecular Devices	N/A
Biorender	Biorender	N/A
GraphPad Prism 5	GraphPad	N/A
Photoshop	Adobe	N/A

RESOURCE AVAILABILITY

Lead contact

Further information and requests for resources and reagents should be directed to and will be fulfilled by the lead contact, Bo Liu (bliu@ucdavis.edu).

Materials availability

Previously reported lines and newly developed transgenic *A. thaliana* lines are listed in the key resources table.

Data and code availability

All data associated with the findings in this paper are included in the main text and supplemental information. There is no original code included in this report. Any additional information required to reanalyze the data reported in this paper is available from the lead contact upon request.

EXPERIMENTAL MODEL AND STUDY PARTICIPANT DETAILS

Arabidopsis thaliana plants used in this study has the genetic background of the Columbia ecotype (Col-0) for the wild-type control, mutants, and transgenic lines. Genotypes associated with different lines are listed in the key resources table. Plants were grown in soil in the controlled growth environment at 21°C under the 16-hr light and 8-hr dark cycle. For live-cell imaging of root tip cells, seeds were sterilized and sowed onto solid media containing ½ Murashige & Skoog media with 0.8% phytagel, followed by 4°C stratification for 2 days prior to being transferred to growth chambers under the identical setting. The roots of 5-day-old seedlings were used for microscopic observations.

Nicotiana benthamiana plants were grown at 25°C with a 16-hr light/8-hr dark cycle. These tobacco plants were grown for 4 weeks prior to agroinfiltration.

METHOD DETAILS

Arabidopsis Mutants and Growth Tests

The myosin MyoXI-4KO mutant and Myosin XI-K-YFP transgenic lines[14] were generously provided by Dr. V. Dolja at Oregon State University, the *trm678, fass5* and TRM7-YFP lines[22] by Dr. D. Bouchez and Dr. M. Pastuglia at Institut Jean-Pierre Bourgin, and the *pok1-1/pok2-3* and YFP-POK1 lines[20] by Dr. S. Müller at Friedrich-Alexander-Universität.

To test oryzalin hypersensitivity, seeds were sterilized and sowed onto solid media containing ½ Murashige & Skoog media with 0.8% phytagel and either 150 nM Oryzalin or equal volumes of DMSO was added for the mock treatment. Seeds were subjected to cold stratification for 2 days before being transferred to the growth chambers and allowed to grow for 23 days.

For microscopic examination, seeds were sterilized and sowed on ½ MS solid media followed by cold stratification for 2 days prior to growth in chamber for 5 days. Seedlings were then transferred to ½ MS solid media containing either 150 nM Oryzalin, 2 μm Lat B, or DMSO for 2 hr prior to live cell imaging or subjection to fixation.

Plasmid Construction and Expression in *Plants*

The MYA1 expression plasmids were constructed in two steps. First, a 6.4-kb genomic fragment, including a 1.3-kb predicted promoter region, was amplified using primers MYA1_Frag1 FOR and MYA1_Frag1 REV. This fragment was inserted into EcoRI-linearized pENTR4 by Gibson assembly to generate pENTR-MYA1F. The second MYA1 genomic fragment was amplified, including the last 4.8kb of the genomic fragment preceding the stop codon, using the primers MYA1_Frag2 FOR and MYA1_FRAG2 REV. It was inserted into pENTR-MYA1F, linearized by MluI, by Gibson assembly to give rise to the full-length genomic construct,

Please cite this article in press as: Huang et al., The microtubular preprophase band recruits Myosin XI to the cortical division site to guide phragmoplast expansion during plant cytokinesis, Developmental Cell (2024), https://doi.org/10.1016/j.devcel.2024.05.015

pENTR-MYA1. The expression vectors were generated by an LR clonase reaction using pENTR-MYA1 and the destination vectors of pGWB4, pGWB16/616, and pGWB559[34,35] which contained the fusion tags of C-terminus eGFP, 4xMyc, and TagRFP, respectively. In addition, pMpGWB123 (Addgene # 68577) was used to introduce a C-terminus 3xCitrine tag to MYA1.

The plasmid, pENTR-TAN1, was made by amplifying a 3.3kb TAN1 genomic fragment, which includes 1.2kb of the predicted promoter region using the primers TAN1_F and TAN1_R. This fragment was introduced into pENTR/D-TOPO by TOPO-Cloning (ThermoFisher). To make TAN1 expression vectors, the pENTR-TAN1 was recombined with either pMpGWB123 or pGWB616 by an LR reaction.

The pCH1-RanGAP1 plasmid was made by amplifying a 2.9-kb RanGAP1 genomic fragment, which includes 1.2kb of the predicted promoter region using the primers RanGAP1_F and RanGAP1_R. This fragment was introduced into pCH1, a modified version of pENTR4 that contains a C-terminus GFP and PA tag, linearized with KpnI and XhoI, through Gibson assembly. To make the expression vector, pCH1-RanGAP1 was recombined with pGWB1.[34]

To make the MYA1$^{874\text{-}1520}$-GFP expression plasmid, a 1.91-kb *MYA1* fragment was amplified from cDNA using the primers I17580_F and I17580_R. This cDNA fragment, encoding a polypeptide of amino acids 874-1520, was inserted into pENTR4, linearized by NcoI and EcoRV, by Gibson assembly. An LR reaction was performed between the resulting plasmid and pGWB6023.[36] The final plasmid allowed us to express MYA1$^{874\text{-}1520}$ fused to a GFP at its C-terminus under the control of the *UBQ10* promoter.

To make the Myosin XI-K$^{881\text{-}1531}$-4xMyc expression plasmid, a 2-kb XI-K fragment was amplified from cDNA using the primers V20490_F and V20490_R. This cDNA fragment, encoding amino acids 881-1531, was inserted into pENTR4, linearized by Nco1 and EcoRV, by Gibson assembly. An LR reaction was performed using the resulting plasmid and pGWB17.[34] The final plasmid allowed us to express Myosin XI-K$^{881\text{-}1531}$ fused to 4xMyc at its C-terminus under the control of the *35S* promoter.

To make the ATK5$^{1\text{-}390}$-GFP expression plasmid, a 1.2-kb ATK5 fragment was amplified from cDNA using the primers ATK5Tail_F and ATK5Tail_R. This fragment, encoding amino acids 1-390, was inserted into pENTR4, linearized by NcoI and EcoRI, by Gibson assembly. An LR reaction was performed between the resulting plasmid and pGWB6023 to give rise to the final expression plasmid.

The MAP65-4-GFP expression vector was previously described previously.[17] The plasmids used to express the tubulin markers, mCherry-TUB6 and VisGreen-TUB6 were reported before.[37] The GFP-SYP111/KNOLLE vector was from an earlier report.[16]

To produce a Myosin XI-K-GST fusion protein in bacteria, the fragment encoding amino acids 1210-1466 included in the cDNA clone 91J23 (Arabidopsis Biological Resource Center at Ohio State University) was cloned into pGEX-4T2 (Millipore Sigma) at SalI and NotI sites. Upon expression, the fusion protein was purified prior to being used as an antigen for immunization in rabbits (Antibodies, Inc).

All expression plasmids were transformed into the agrobacteria strain, GV3101, prior to *A. thaliana* transformation by floral dipping or transient expression by agroinfiltration in tobacco leaves.

Immunoprecipitation and Immunoblotting Analysis

Proteins were extracted from flower buds of transgenic *A. thaliana* plants. Approximately 4 g of floral tissue was collected and extracted in the extraction buffer containing 50 mM Tris-HCl pH 8, 150mM NaCl, and 1% Triton X-100, supplemented with EDTA-free protease inhibitor. The sample was centrifuged at 10,000-RPM (24,300g) in an Avanti J-25I centrifuge (Beckman Coulter) for 20 minutes. The soluble fraction was added with 50 μl of anti-GFP magnetic MACS microbeads (Miltenyi Biotec) and incubated for 40 minutes. The fraction was loaded to magnetic μ column and proteins were eluted with 70 μl of elution buffer (Miltenyi Biotec). Protein samples were separated by SDS-PAGE and transferred to PVDF membrane using the Turbo Transfer System (Bio-Rad). Immunoblotting was performed by first hydrating PVDF membrane in methanol, followed by incubation in blocking buffer containing 3% BSA in 1X TBST for 1 hr. Membrane was washed with 1X TBST, and primary antibodies were then added to the membrane for 3 hrs. Primary antibodies included rabbit anti-Myosin XI-K against the fusion protein described above, rabbit anti-c-Myc (Millipore Sigma), and rabbit anti-GFP.[38] Membrane was washed with 1X TBST prior to incubation with the secondary HRP-conjugated goat anti-rabbit antibodies for 1hr. Membrane was washed with 1X TBST. Chemiluminescence was performed by adding the substrate mix containing 1:1 volume ratio of Clarity Western Peroxide Reagent and Clarity Western Luminol/Enhancer Reagent (Bio-Rad). The substrate was added to the membrane immediately prior to having the blot imaged under a ChemiDoc System (Bio-Rad).

To identify interacting CAMP proteins, co-IP experiments were performed similarly as described above by using *A. thaliana* floral tissues. The soluble fraction was mixed with 200 μl of anti-GFP microbeads and eluted with 190 μl of elution buffer. Protein samples were loaded onto SDS-PAGE gel and the resolving gel containing the isolated proteins were cut and subjected to trypsin digestion prior to LC-MS-MS analysis for protein identification at the Taplin Biological Mass Spectrometry Facility at Harvard Medical School.

To test interactions between truncated Myosin XI fragments, we performed co-IP experiments using lysate from *N. benthamiana* leaves that had these fragments transiently expressed. Agrobacterial cells were grown in liquid LB medium to stationary phase. Bacterial cells were collected by centrifugation and resuspended in 10 mM MES (pH 5.6) buffer containing 10 mM $MgCl_2$ and 150 μM acetosyringone to an OD_{600} of 1.0. A separate agrobacterial strain carrying the p19 expression plasmid was included to suppress gene silencing.[39] Bacterial cells were then mixed together at equal volumes and injected into 4-week-old *N. benthamiana* leaves. Plants were placed back into growth chambers to recover and grow for 3 days. On the third day, leaves were collected for protein extraction and immunoprecipitation following the protocol described above.

Please cite this article in press as: Huang et al., The microtubular preprophase band recruits Myosin XI to the cortical division site to guide phragmoplast expansion during plant cytokinesis, Developmental Cell (2024), https://doi.org/10.1016/j.devcel.2024.05.015

CellPress

Analysis of co-purified proteins from mass spectrometry

Peptides detected by mass spectrometry were referenced to the *A. thaliana* proteome of TAIR11 (https://www.arabidopsis.org) for the identification of corresponding gene. Three biological replicates of YFP-POK1 purification and three GFP purifications serving as the negative control. The genes/proteins presented in Figure 3A were selected by using the GO terms of cytokinesis by cell plate formation, microtubule-based movement, actin filament-based movement, and preprophase band, which were identified by using PANTHER (https://go.pantherdb.org/). The presences of proteins co-purified with YFP-POK1 was tallied out of three trials and displayed by using a heatmap.

Indirect Immunofluorescence and Confocal Microscopy

To label the outline of root cells, 23-day old seedlings grown on solid media was soaked in 20 μg/mL propidium iodide for 1 min. Following a brief rinse with water, the roots were immediately imaged under an LSM710 laser scanning confocal equipped with a 40X water immersion objective (Carl Zeiss).

For immunofluorescence microscopy, *A. thaliana* roots were fixed and squashed on slides following previously established protocol.[40] Fixed cells were imbedded with primary antibodies in different combinations. The antibodies and dilutions are as follows, 1:400 DM1A mouse anti-α-tubulin and 1:400 polyclonal anti-c-Myc (Millipore Sigma), 1:400 polyclonal rabbit anti-GFP, 1:200 monoclonal mouse anti-c-Myc (DSHB at University of Iowa), 1:200 sheep anti-tubulin (Cytoskeleton, Inc.), and 1:1000 monoclonal rat anti-PA (FUJIFILM Wako Pure Chemical Corp.). Secondary antibodies included fluorescein isothiocyanate (FITC)-conjugated donkey anti-rabbit, Texas Red-conjugated goat anti-mouse, Texas Red-conjugated donkey anti-goat (Rockland Immunochemicals), Alexafluor 568-conjugated goat anti-mouse, Alexafluor 488-conjugated goat anti-rabbit (Thermo Fisher), all diluted 1:400. Nuclei were marked by staining DNA with 1 μg/mL DAPI. Slides were mounted with either Slowfade or Prolong Glass (Thermo Fisher). Cells were observed under an Eclipse 600 epifluorescence microscope equipped with a Plan-Fluor 100X objective (Nikon).

Live-cell imaging of fluorescent protein-labeled target proteins described above in *A. thaliana* seedlings was performed by using a 40X water immersion or a 100X oil immersion objective attached to the LSM710 and LSM980 Airyscan2 confocal microscopes. STED was performed using a 100x oil immersion objective on a Leica TCS SP8 STED 3X microscope. Images were processed by using the Metamorph software (ThermoFisher), ImageJ (https://imagej.nih.gov/ij/),[41] Zen (Black Edition), Leica Application Suite X, and Huygens Professional.

Analysis of Root Growth and Plane of Division

Seeds were sowed and grown on ½ MS solid media supplemented with either oryzalin or DMSO, as stated above. Roots were measured after 23 days.

Cells from the root meristematic zone were used for the measurement of cell wall angles. The extracellular space between cell walls were labeled using propidium iodide. The angle was measured between the transverse cell walls and the adjacent longitudinal cell wall on the side closest to the epidermis. The cells of the epidermis and cortex were included in the measurement because of their larger sizes and clearly defined boundaries between cells.

Quantification of Collapsed Spindles

Arabidopsis seeds were sowed and grown on ½ MS solid media and allowed to grow for 5 days. Seedlings were transferred to supplemented with. Meristematic root cells of 5-day old seedling were treated with ½ MS solid media containing 150 nM oryzalin or DMSO for 2 hrs prior to fixation and anti-tubulin immunostained by following the protocol described above. Collapsed spindles that lacked bipolarity and had clustered kinetochore fibers were counted from total meristematic root cells at mitosis.

Analysis of Cortical Foci

Immunofluorescence images of root cells undergoing cytokinesis was used for analyses of cortical patterns. Colocalization of different CAMP proteins was analyzed graphically by first finding the maximum signal at the cortex and defining those as foci. The image was filtered using a Guassian filter tool and then binarized. Signal intensity was determined by drawing a line scan across the cortex of the cell. The signal intensities of both proteins were normalized by min-max normalization. To quantify the pattern of the cortical foci, the axial plane of the cell was used. Maximum intensity of signal along the cortex was used to define the centroid of the foci. The distance between the adjacent foci was calculated by drawing a line from the centroid of one focus to the centroid of adjacent focus along the cortex. Each individual distance value was divided by the perimeter to display the percentage of the perimeter that each pair of foci occupied. Manders' colocalization coefficient between CAMP foci was calculated by using the JaCoP plugin in ImageJ.[42]

To qualify the occupancy of TAN1 in myosin mutants, the centroids along the cell cortex was determined based on maximum intensities along the perimeter. The images were binarization to normalize the intensities. The perimeter section occupied by TAN1 is divided by the total perimeter to display the percentage occupancy.

To quantify the MYA1 cortex lateral diffusion after Lat B treatment, the width of foci along the cortex was measured on both sides of the cell. For each cell, the focus width at both sides of the cell was averaged then divided by the perimeter. To quantify the axial plane after Lat B treatment, the image was first binarized to normalize signal intensities either 1 or 0. A line was drawn across the cell cortex and signal intensities cross the cortex were obtained. The area with signal intensity of 1 was divided by the total area to give us the percentage of area occupied by foci.

Please cite this article in press as: Huang et al., The microtubular preprophase band recruits Myosin XI to the cortical division site to guide phragmoplast expansion during plant cytokinesis, Developmental Cell (2024), https://doi.org/10.1016/j.devcel.2024.05.015

QUANTIFICATION AND STATISTICAL ANALYSIS

Microscopic images were quantitatively analyzed in ImageJ. Statistical tests, significance and sample size are presented in the figure legends.